fire

MDPI

Article

A Framework for Conducting and Communicating Probabilistic Wildland Fire Forecasts

Janice L. Coen [1,2,*], Gary W. Johnson [3], J. Shane Romsos [3] and David Saah [1,3]

[1] Department of Environmental Science, University of San Francisco, San Francisco, CA 94117, USA; dssaah@usfca.edu
[2] NSF National Center for Atmospheric Research, P.O. Box 3000, Boulder, CO 80307, USA
[3] Spatial Informatics Group, 2529 Yolanda Ct., Pleasanton, CA 94566, USA; gjohnson@sig-gis.com (G.W.J.); sromsos@sig-gis.com (J.S.R.)
* Correspondence: jcoen@usfca.edu; Tel.: +1-(303)-497-8986

Abstract: Fire models predict fire behavior and effects. However, there is a need to know how confident users can be in forecasts. This work developed a probabilistic methodology based on ensemble simulations that incorporated uncertainty in weather, fuel loading, and model physics parameters. It provided information on the most likely forecast scenario, confidence levels, and potential outliers. It also introduced novel ways to communicate uncertainty in calculation and graphical representation and applied this to diverse wildfires using ensemble simulations of the CAWFE coupled weather–fire model ranging from 12 to 26 members. The ensembles captured many features but spread was narrower than expected, especially with varying weather and fuel inputs, suggesting errors may not be easily mitigated by improving input data. Varying physics parameters created a wider spread, including identifying an outlier, underscoring modeling knowledge gaps. Uncertainty was communicated using burn probability, spread rate, and heat flux, a fire intensity metric related to burn severity. Despite limited ensemble spread, maps of mean and standard deviation exposed event times and locations where fire behavior was more uncertain, requiring more management or observations. Interpretability was enhanced by replacing traditional hot–cold color palettes with ones that accommodate the vision-impaired and adhere to web accessibility standards.

Keywords: wildfire modeling; ensemble; uncertainty; fire behavior; forecasting; prediction; coupled weather–fire model; fire effects modeling; ensemble visualization; web accessibility

Citation: Coen, J.L.; Johnson, G.W.; Romsos, J.S.; Saah, D. A Framework for Conducting and Communicating Probabilistic Wildland Fire Forecasts. *Fire* **2024**, *7*, 227. https://doi.org/10.3390/fire7070227

Academic Editor: Hans Pasman

Received: 28 April 2024
Revised: 24 June 2024
Accepted: 26 June 2024
Published: 1 July 2024

1. Introduction

Land management today is exceedingly complex, with key difficulties in assessing and managing uncertainty to limit wildland fire risk. It aims to mitigate the extent and impact of wildfires that are said to be becoming more unpredictable [1] and which are often characterized by complex, uncertain behavior in steep, complex, and forested terrain. This is weighed against the strategic manipulation of forest fuel amount and structure using tools such as prescribed fire, which is accompanied by its own risks [2]. Retrospectively, inadequate evaluation of fire and weather conditions is often cited in cases of unintended prescribed fire consequences [3]. Uncertainty about fire effects, such as the smoke impacts of prescribed fire, also reduces its use [4]. Mitigation now requires quantitative planning [5] but modeling tools do not currently have the dynamic complexity and means to estimate confidence in predicted fire behavior, smoke, and ecological effects, especially in complex environments [6,7]. The benefits of better estimating uncertainty extend to improving firefighter safety, as entrapment potential peaks when fire behavior rapidly deviates from an assumed trajectory and becomes extreme [8].

To date, forest and emergency management planning have accessed deterministic kinematic models. Used as guidance, deterministic prediction of both wildfire and prescribed fire behavior and effects has shown limitations, particularly in outlier events [9]. Examples

of fire behavior prediction tools in the United States include FARSITE [10], Minimum Travel Time (MTT) [11], Near Term Fire Behavior in the Wildland Fire Decision Support System [12], Wildfire Analyst [13], WIFIRE [14], ELMFIRE (Eulerian Level Set Model of Fire Spread) [15], and GridFire [16], each built using U.S.-based semi-empirical fire algorithms. To some extent, shortcomings arise from one of this kinematic model generation's now-recognized limitations—its inability to represent fire-induced winds created by the fire's interaction with the surrounding atmosphere—and thus overlook the potential for dynamic feedbacks, and amplification into sudden shifts in wind and fire direction, blow-ups, and large fire whirls. Thus, many kinematic models in use today can underestimate the range of possible outcomes, leading to the misinterpretation of possible impacts to people, property, and the environment.

Transient fire behavior and phenomena have been better modeled and, when used to forecast fire spread, better predicted by a new generation of dynamic coupled numerical weather prediction (NWP)–wildland fire behavior systems (hereafter referred to as "coupled models"), some of which are being tested in operational forecasting frameworks (e.g., CAWFE® [17], WRF-Fire [18], and their derivatives). Although coupled models should be able to simulate transient, dynamic behavior arising from internal dynamics (e.g., surprising fire runs on days similar to previous weather, blow-ups, destructive fire whirls, and plume-driven behavior such as the production of pyrocumulus and plume collapse), a wide range of outcomes are possible given very similar initial conditions because of the inherently nonlinear, apparently unpredictable nature of wildfire events. Other dynamic models (e.g., FIRETEC [19], WFDS [20,21], QUIC-fire [22]) are used non-operationally at meter scales for fuel treatment or prescribed fire decision-making. Although the more sophisticated generation of dynamic fire models may reproduce higher fidelity and complexity, the need to calculate and communicate the uncertainty associated with fire prediction becomes even more critical.

Recognizing the practitioner's need for confidence estimates related to fire forecasts, efforts have been made to attach uncertainty estimates to fire behavior predictions [23]. These are meant to answer questions such as: "How confident are you in your prediction? 90%? 50–50?", "What is the range of possible outcomes?", or "What outcome is most likely?" Current efforts to bridge this gap include industry standard tools such as Fire Spread PRObability simulator (FSPro) [24], which draws from climatology and its variability at a current fire's location to estimate a range of possible outcomes. A drawback is that the past is not necessarily a good prediction for current conditions, especially in outlier situations. In addition, in practice, interpretation of FSPro graphical predictions for probability of being burned over can easily be misinterpreted as the deterministically predicted shape of an expanding fire perimeter. Fresh approaches are needed that answer user demands for fire behavior and associated fire effects forecasts that include clear and meaningful information about how confident one can be in them. However, human impact research on the issuance of weather forecasts that are statistical in nature (e.g., "a 50% chance of rain", "a 100-year flood") has shown that people interpret such information differently [25] and not always as intended. Thus, to be valuable, an approach must effectively convey how users should interpret its products.

This study developed and applied an approach for conducting and communicating probabilistic fire growth forecasts that can be used with a wide range of fire behavior modeling systems. It carried the uncertainty in key fire environment input variables—notably, weather and fuel loads— and physics parameters through to estimate uncertainty in predicted outcomes of fire behavior and effects using four coupled weather–wildland fire model ensemble simulations of recent wildfire events. It also developed methods to graphically and effectively communicate to a wide range of practitioners the probabilistic fire growth forecast uncertainty but also the operationally relevant rate of spread and an example of a fire effect, fire heat flux, as an indicator of fire severity.

2. Background

This approach draws from several disparate research threads in its aim to satisfy both a research and application gap; a summary of each follows. This section describes user needs, the status of probabilistic fire growth, weather, and fuel products, and research on visualization of ensembles.

2.1. User Needs

The disconnect between users' needs and current wildfire model products reflects both a recognition that model predictions are often imperfect and users' discomfort with probabilistic information, which is often considered "hedging". While a single deterministic simulation is relatively simple to convey, it will likely contain error. While Gaussian (normal) distributions are often assumed to be the outcome of an ensemble of simulations, probabilistic forecasts can produce a variety of fire perimeter shapes [26] (Figure 1). A narrow range of outcomes can mean one is relatively confident in the forecast quantity while a wide range can indicate confidence is low. The distribution can be skewed when outcomes on one side are more likely than the other, or when the uncertainty is bimodal or has extended tails.

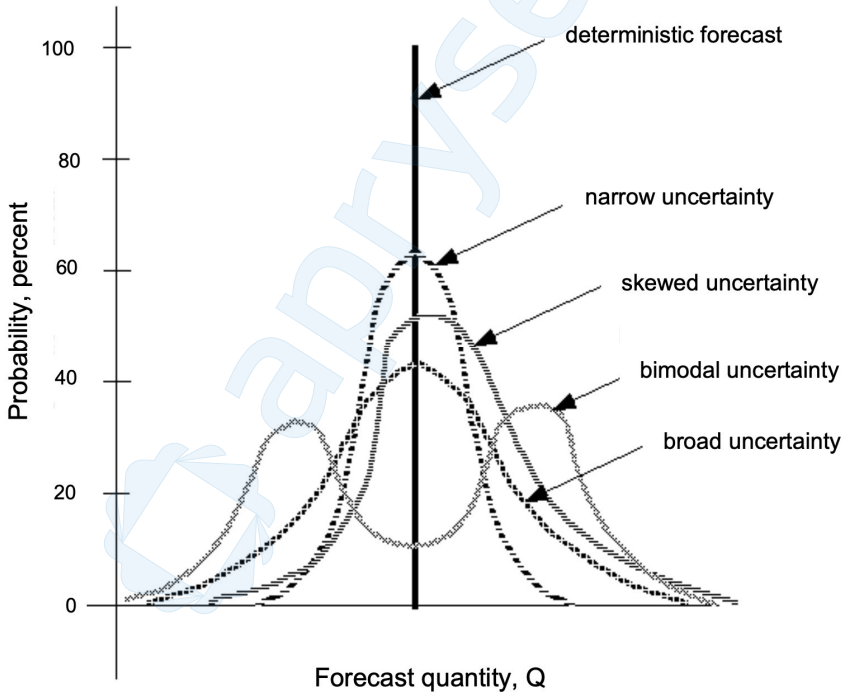

Figure 1. Examples of different types of uncertainty outcomes. Modified from [26].

Improbable, highly destructive "black swan" events [27] that arise from "a perfect storm" of fatally timed components are easily missed by single deterministic simulations. Errors in one input (such as forecasted wind speed or direction) can result in spurious fire predictions. Large wildland fires are driven by spatially and temporally varying heat fluxes released by burning vegetation, creating updraft plumes, wind shifts, firenadoes, pyrocumulus clouds, and other transient phenomena. The least understood events and phenomena arise from complex mountain airflows, plume-driven fires, fire-induced winds, and situations where both play a role. An example of the latter is the Carr fire behavior on 26 July 2018, where the growing wildfire overran the shifting intersection of two airflows—westerlies descending into the Sacramento Valley creating a confluence line with dry southerlies—just as it entered Redding, spinning up a large, destructive fire vortex with winds exceeding 50 m s^{-1} seen in radar data [28] and modeling [29]. In addition to scientific

issues in reproducing such events, outliers present a communication challenge—how to communicate the small possibility of a catastrophic event.

Finally, a key need for land managers is the ability to predict fire effects, such as smoke production, various severity metrics, and mortality, in a physically consistent manner with fire behavior [30], rather than diagnosing fire effects with separate models using unmeasured or unknown fire behavior metrics, as is currently done. A parallel need is to estimate the error in those fire effects predictions due to uncertainty in environmental conditions, notably weather and fuel. For example, air quality managers currently are presented with multiple different predictions of smoke impacts with no confidence or uncertainty estimates, making it difficult to use this information for guidance.

2.2. Probabilistic Fire Growth

Operational fire prediction is founded on deterministic prediction for short-term estimates of fire growth and, recognizing the increasing unreliability in longer-term predictions due to decreases in weather forecast skill with time, seeks to express the possible range of outcomes for longer-term fire forecasts [12]. This section describes approaches in which fire models are used to estimate the range of possible outcomes, and although it makes a key distinction between two classes of models, it does not detail specific models' limitations. (Note that in fire modeling literature, the term "uncertainty" has sometimes been used to refer to a particular model's error rather than an estimate of confidence.)

Though multiple efforts have used multiple simulations to estimate a range of possible outcomes, there is currently no established consensus or state-of-the-art approach to constructing fire modeling ensembles (i.e., how many simulations to run or how to make members different from each other) themselves. In addition, previous efforts have used kinematic (e.g., [31,32]) rather than dynamic models. Kinematic models focus more on the motion of fire spread without considering complex interactions between variables. Dynamic models, on the other hand, incorporate nonlinear interactions between different factors, such as fire–weather feedbacks. Only in the latter can small perturbations in initial conditions amplify through nonlinear interactions between variables where, over time, the amplified errors lead to diverging forecasts (the "uncertainty"), where the difference between the actual state and the predicted state (the model error) grows with time.

The operational FSPro simulator [24] calculates fire growth from the current extent using the kinematic model FARSITE, wind velocities stochastically sampled from historical observations from a nearby weather station (i.e., climatology), seasonal trends in fuel moisture, and recent weather trends to produce fire growth forecasts for two weeks or more [12]. FSPro calculates two-dimensional fire growth and maps the probability of a fire reaching each point on the landscape in the determined time interval (e.g., the next two weeks). This approach has weaknesses that lead to unsatisfactory predictions. Namely, it assumes that historical wind variability indicates the conditions and the uncertainty in the near future, whereas a sample of past conditions may not reflect more extreme conditions driving the current fire. Other probabilistic modeling approaches borrow the numerical weather prediction term "ensemble" [33] to describe the use of many simulations. Past efforts have generated longer-term probabilistic predictions from wind station data based on the likelihood of past wind regimes [34] or other atmospheric state variables [35]. Others simply varied inputs over the natural possible range of input fire environment variables—for example, ref. [36] used the natural range of fuel loads to compute a range of possible outcomes as if each were equally likely, while others arbitrarily assigned probability to inputs [37]. While these approaches may produce a suite of naturally possible outcomes, each member of the set of simulations is not equally likely and when considered as a whole, the frequency of an outcome does not represent its probability of occurrence. As a result, the spread among the outcomes in these approaches does not answer the critical questions of how uncertain current conditions are, which outcome is most likely, or how confident one should be.

Visual presentation of fire growth forecasts has similarly been limited to static presentation of the probability of being overrun during a particular period. The expansion of internet-delivered information, the variety of device capabilities, and need for web accessibility compliance to support disability inclusion in the workforce call for a renewed approach to communicating needed uncertainty information. Color palettes commonly used in earth system modeling (e.g., red/hot–green/cold, or blues/yellows) are difficult to discern by those with the most common types of color blindness, while accessible color palettes aim for higher standards (e.g., maintaining contrast), considering how those with other vision impairments will perceive web content. Importantly, as products may be adopted by federal or state agencies, associated products must meet web accessibility compliance standards established for those working with federal and many state governments such as 508 compliance [38] or Title III of the Americans with Disabilities Act, accommodating individuals with disabilities (e.g., color blindness) so that they may interact with new technology.

2.3. Probabilistic Weather Forecasts

Numerical weather prediction research has grappled with forecast uncertainty. The atmosphere is a nonlinear dynamical system that depends sensitively on the initial conditions. Estimates of the current state and the models themselves are imperfect; thus, forecast uncertainty grows with simulated time. One way to explicitly address uncertainty is using ensembles of simulations [39] rather than single deterministic forecasts. Dynamic ensemble forecasts are composed of multiple "ensemble members"—independent forecasts that are configured in a unique manner to provide forecast diversity. This diversity can be achieved by configuring individual members with different meteorological initial conditions, inputs, or physics. Due to these differences between members' configurations, forecast outcomes across the members will differ, and the range of outcomes predicted by an ensemble indicates uncertainty and is related to forecast confidence. Furthermore, probabilities of event occurrence can be easily calculated. Compared to single deterministic forecasts, probabilistic forecasts offer more information to users and can aid decision-making (e.g., [40]). However, ensemble numerical weather prediction comes with several limitations including computational cost, biases inherent to their underlying weather models, limited spread and independence among members and outcomes, and struggles to predict rare or extreme events, along with verification challenges, interpretation, and communication [41].

High-resolution ensembles have increasingly been used in NWP and are now run in real time at many worldwide centers, including the National Centers for Environmental Prediction's (NCEP) High-Resolution Ensemble Forecast (HREF) system and the Short-Range Ensemble Forecast (SREF) weather forecast system. SREF is a regional ensemble operated over North America. It provides an 87 h forecast with output at 3 hourly intervals using a 16 km horizontal grid spacing initialized at 0300, 0900, 1500, and 2100 Coordinated Universal Time (UTC). It has 26 members: 13 use the Advanced Research WRF (WRF-ARW) model and 13 members use the NEMS Non-Hydrostatic Multiscale Model on a B-grid (NEMS-NMMB). These SREF ensemble members use different physics parameterizations, lateral boundary conditions from the Global Ensemble Forecast System (GEFS), and initial conditions to generate variability between members. Details on the various SREF members can be found in [42].

The variability in predictions between ensemble members increases with time, between atmospheric state variables, and between weather types. For example, Figure 2 shows predicted precipitation, temperature, and near surface winds from SREF forecasts for two different conditions—a summer day with little precipitation (Figure 2a–c) and one with convective rainfall (Figure 2d–f). The presence of precipitation dramatically increases the difference between members, and even when temperature spreads little between members, differences in near surface winds increase with time. As gridded output from ensemble forecasts such as SREF may be used as initialization and boundary condition data for more refined simulations, a hypothesis is that this uncertainty in weather input encapsulates

the possible fire behavior outcomes. Thus, because wind is the most important factor influencing fire growth rate—rate of spread responds as much as the square of the wind speed in some flashy fuel types—it is anticipated that variance among SREF members could amplify variability in predicted fire spread.

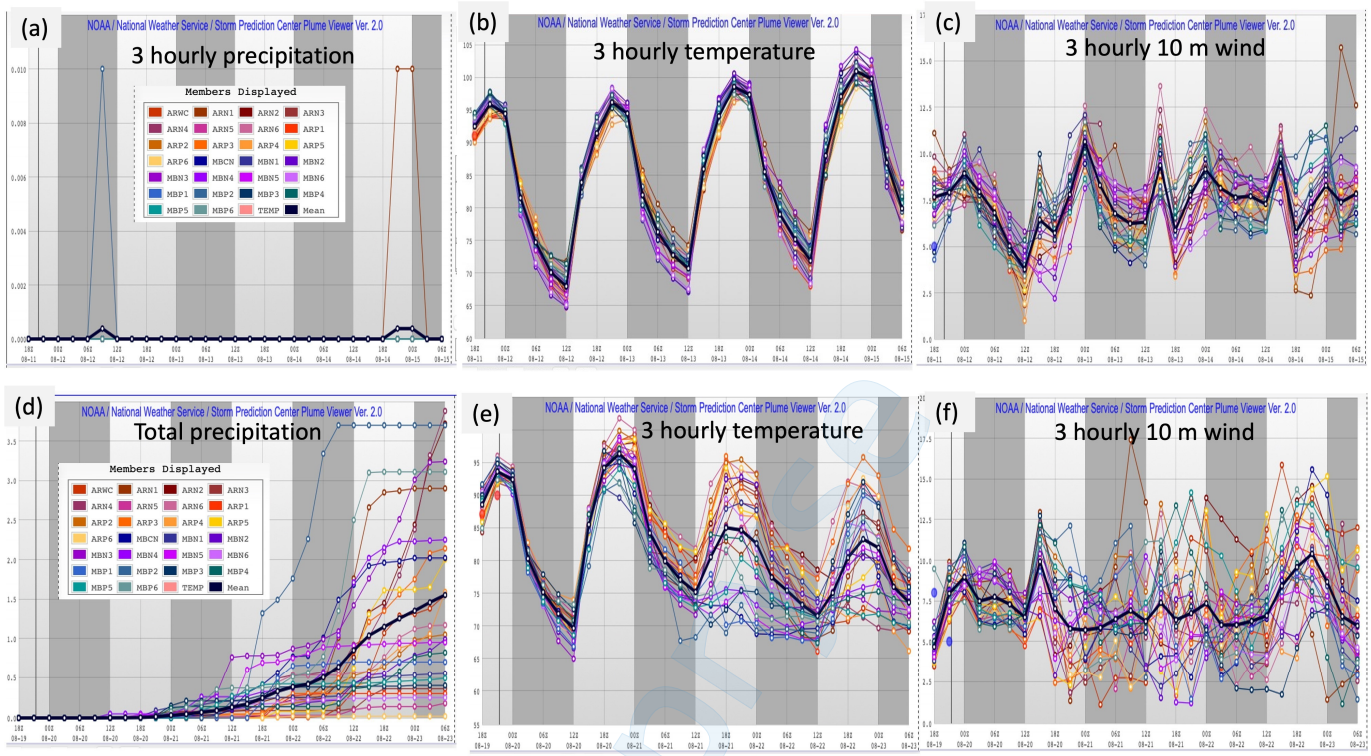

Figure 2. NCEP SREF forecasts for Oklahoma City (OKC) for 2 days with different weather types: 11 August 2022, at 15 UTC, a day with little precipitation (upper row) and 19 August 2022, at 15 UTC, a day with convective precipitation (lower row). The forecast fields are (**a**) 3 hourly precipitation, (**b**,**e**) 3 hourly temperature, (**d**) total cumulative precipitation, and (**c**,**f**) 3 hourly 10 m wind speed. Figures obtained from [43].

2.4. Probabilistic Fuel Information

Many fire modeling systems rely on the United States Geological Survey's LANDFIRE database, which offers fuel data wall-to-wall across the U.S. LANDFIRE provides fuel information through stylized categorical surface fuel models (e.g., [44,45]), enabling modeling of fire behavior, emissions, and other fire-related products. Each surface fuel model prescribes a characteristic load (mass per unit area), depth, surface area to volume ratio, and physical characteristics. Additional data layers provide canopy load, base height, and height. Advances have been made in documenting errors in LANDFIRES's fuel types [46] but the methodology has limitations, e.g., its data is largely static, updated on a several-year rotation, and it provides a single set of characteristics based on the ecosystem type whereas a broad range of site conditions, such as stand age, geographic conditions, and other factors introduce large variations in fuels even within one mapped fuel type [47].

Recent advancements in fuel measurement include the development of methods using LiDAR remote sensing data to infer fuel type and structure from airborne or terrestrial platforms. LiDAR offers detailed 3D views of vegetation, resulting in more accurate fuel estimates compared to methods reliant on manual sampling and which potentially diverge from standard forest databases like LANDFIRE (e.g., [48,49]). Airborne LiDAR has given insight into fuel characteristics (crown bulk density, height to live crown, ladder fuels biomass, and in some conditions, surface fuels biomass) (e.g., [50]). However, advances in remote sensing approaches to fuel measurement stem largely from the sensitivity of small-

footprint terrestrial LiDAR to understory conditions, whereas airborne remote sensing is primarily sensitive to the upper canopy, leading to potential errors. Still, the error or "uncertainty" in products derived from these measurements or the standard databases is not provided or known. While the accumulation or deliberate reduction in fuel loads is widely credited with modulating fire behavior across many ecosystem types, given that simulated fire behavior using coupled models has shown dramatically different sensitivities than previous kinematic models to fuel properties through the possibility of "plume-driven" dynamic feedbacks in complex terrain [51,52], variability in predicted fire behavior between ensemble members may be amplified in coupled model ensembles where fuel uncertainty is used to establish the ensemble member configuration.

The assemblage of fuel datasets from LiDAR, other techniques, and direct field measurements have allowed researchers to develop more sophisticated databases that not only provide the mean properties for a particular fuel type but also provide a probability density function representing the inner-category variability. The North American Wildland Fuels database (NAWFD) was created to improve characterization of fuel loading for types across the U.S. [47]. The database is a compilation of fuels data from many sources and provides a new fitted distribution of loadings for each fuel bed strata (Figure 3) [46].

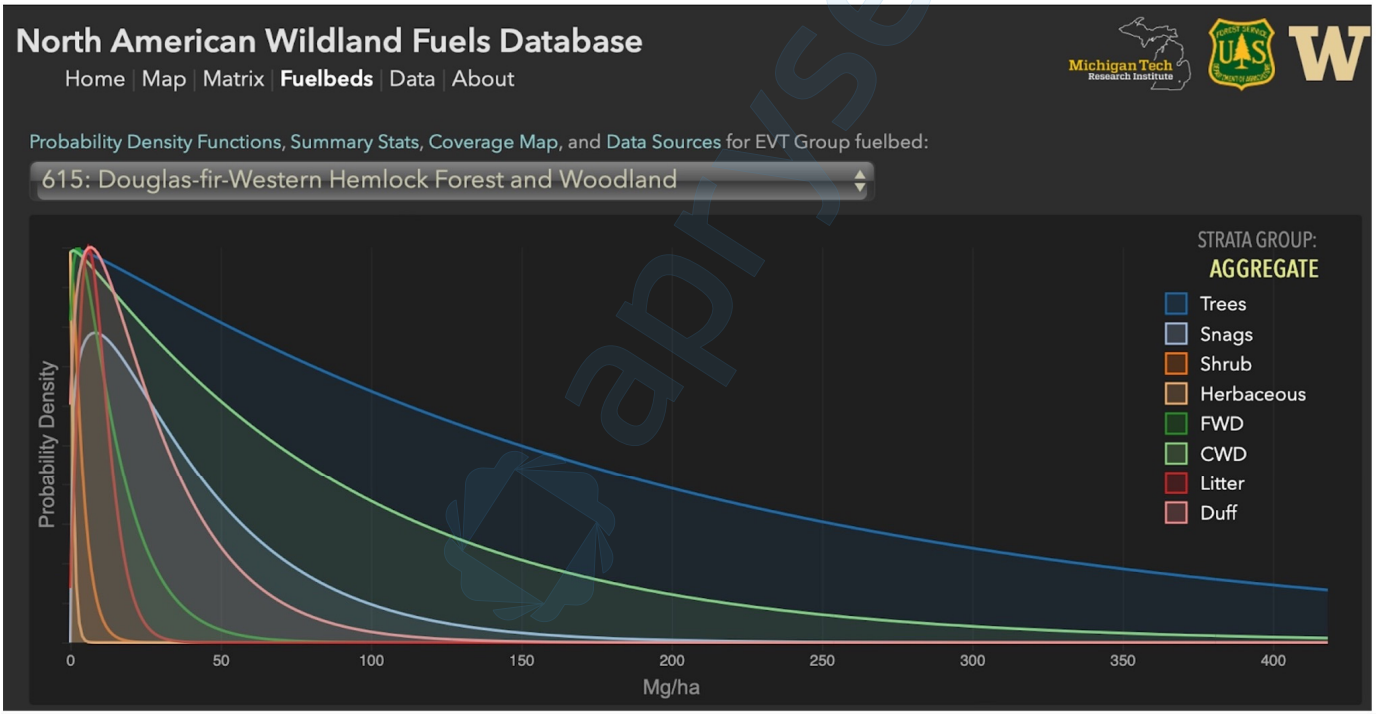

Figure 3. Example of the NAWFD fuel bed view for the Douglas fir—western hemlock existing vegetation type (EVT), showing computed probability density functions for each fuel bed stratum. Figure was generated using https://fuels.mtri.org.

2.5. Visualization of Ensembles

Methods for visualizing ensembles have advanced along with the availability of ensemble datasets and expansion of ensemble use across disciplines [53]. In [53], authors reviewed how traditional visualization techniques have been adapted to meet the challenge of visualizing data with an additional dimension (the number of members), categorizing research by technique and the analytic task (e.g., comparison, clustering, or trend analysis). Other examples of visualizing ensembles include [54], which developed an approach to visualize confidence in cluster-based analyses of trends in ensemble weather forecasts, visualizing the robustness of clusters and uncertainty in trends. Also, Ref. [55] presented a method to visualize the statistical properties of streamlines passing through a location

from an ensemble of flow fields. In the latter, derivation of confidence regions indicated where streamlines most likely reside [55].

Color mapping is a crucial aspect of data visualization, enabling users to successfully and efficiently glean insights from data [56]. A survey on techniques for generating color maps [56] categorized these methods based on the characteristics of the data in various applications, providing a reference for users dealing with similar data or tasks. In [57], color theory concepts were applied to digital media and visualization, visual color impairments were reviewed, and tools were provided for examining how a specific color map will look to affected individuals.

3. Materials and Methods

This study applied the ensemble approach, widely used in meteorology, to coupled weather–fire modeling to communicate the range of possibilities in predicted fire products (fire progression, the operational criterion of spread rate, and heat flux, which may be related to vegetation burn severity, an example of a fire effect) due to uncertainty in the principal factors of weather, fuels, and physics parameters. Ensembles were constructed such that in each, the breadth of the solutions reflected the uncertainty from each source (either weather, fuel load, or physics parameters). Visualization techniques were developed to communicate likely outcomes, confidence, and areas or times of uncertainty or outlier behavior.

3.1. The CAWFE® Coupled Weather–Wildland Fire Behavior Model

CAWFE® (derived from Coupled Atmosphere–Wildland Fire Environment) integrates an NWP model with a module for fire behavior and fuel consumption. These components interact, with heat and water vapor fluxes from the fire influencing the atmospheric state, resulting in fire winds. Conversely, the evolving atmospheric conditions impact fire behavior. CAWFE is built upon a 3D meteorological model [58,59] optimized for fine scales (~100 m grid spacing) in extremely complex terrain. Vertically stretched terrain-following coordinates allow detailed simulation of airflow at horizontal resolutions of tens of kilometers while telescoping in to focus at hundreds of meters. The outer of several interactive, nested modeling domains is initialized from and boundary conditions are updated with gridded atmospheric analyses or large-scale model forecasts, such as the members of the SREF.

CAWFE's fire module [17,60] uses semi-empirical algorithms to calculate the speed of surface fire spread within wildland fuel complexes [61]. This prediction is based on terrain features, fuel characteristics, moisture levels, and fire-altered winds. Additionally, the module estimates fuel consumption rates, whether fire transitions into the canopy, and the subsequent spread as a crown fire [62]. The consumption of fuel is determined using BURNUP [63] algorithms. As the fuel is consumed (data sourced from LANDFIRE [64] or the North American Wildland Fuels database (NAWFD), detailed below), it releases sensible and latent heat, as well as smoke particulates, dispersed throughout the lowest atmospheric grid volumes. These algorithms represent fire and fuel properties on a subgrid within each atmospheric cell at ground level. Fires may be introduced into a simulation either using ignition location and time or in progress using active fire detection data from the Visible and Infrared Imaging Radiometer Suite (VIIRS) [65] or Landsat's Operational Land Imager (OLI) [66] sensors, incident reports, or airborne fixed wing or UAS data, all of which can also be used for evaluation.

As configured here for a forecast, CAWFE operates with a 370 m horizontal grid spacing, running approximately 6 times faster than real-time on a single workstation processor for large events (e.g., [51,67]) and 20 times faster for small fires; thus, this approach can be applied as a forecasting system.

3.2. Overview of Experiments

Four ensemble simulations using CAWFE were performed to capture a spectrum of wildfire behaviors across diverse environments. The events were selected because they

were shaped by distinct drivers. Specifically, wind-driven fires are sensitive to topographic airflow parameters while plume-driven fires are driven by fire-induced winds fueled by fuel consumption, and thus, are sensitive to fuel loads. As a test, these experiments provided the greatest opportunity for small differences to grow and drive members apart.

These ensembles simulated up to 36 h periods of three events. One was a period of the Mosquito Fire, California's largest wildfire of 2022, when it experienced plume-driven growth within the canyons of the American River watershed, occurring amid dry conditions and weak ambient winds [68]. This employed both physics-varying and SREF weather initiation ensembles.

A second ensemble was applied to the 2017 Tubbs Fire, which occurred during a strong Diablo wind event and was one of more than two hundred wind-driven fires that occurred during the 2017 California North Bay firestorm [69]. Previous studies of this event (e.g., [67]) noted the presence of pulsing winds and wind extrema over shorter, secondary ridges—an exceptional airflow regime produced by a shallow river of fast moving, stable air near the surface. This ensemble used a weather-varying initialization from the SREF mesoscale weather forecasting ensemble. Varied weather inputs are important in downslope wind events because subtle differences in the modeled airflow, particularly wind speed at hilltop height, can generate vastly different flow patterns and wind maxima. These fluctuations can profoundly alter the behavior and spread of fires in such environments.

The third event modeled was the 2021 Caldor Fire [70], a wildfire southwest of Nevada/California's Lake Tahoe, that was driven jointly by moderate ambient winds and upslope plume-driven winds [71], as seen on ALERT California camera feeds [72], during this period. This ensemble was initialized with varying fuel conditions. The sensitivity to fuel loads was of particular significance in this case because prior partial fuel reduction was carried out to reduce fire danger to the community of Grizzly Flats, which was overrun by the Caldor Fire during this period [73]. While sensitivity to weather was also important, the SREF mesoscale ensemble forecast data are typically not archived longer than a week and were not available for the simulated period.

In each simulation, CAWFE was configured with 4 nested domains, refining from 10 km horizontal grid spacing by a horizontal refinement ratio of 3 to 3.33 km, 1.11 km, and 0.370 km. In simulations of the Mosquito Fire and Caldor Fire, the vertical grid was refined by a factor of 2 in the 4th domain, and, in the Tubbs simulation, the vertical grid was refined by a factor of 2 in the 3rd domain and by another factor of 2 in the 4th domain.

3.3. Physics-Varying Ensemble Forecast of the Mosquito Fire

The 17-member physics-varying CAWFE ensemble began with a control experiment (MQ01), around which various parameters were systematically altered. These parameters included fuel properties (such as load and depth, dead fuel moisture content, or canopy moisture content), the method and vertical location for sourcing winds that drive the fire, model smoothing parameters (e.g., length scale for the model smoothing coefficient or strength of a model filter (VIS)), and parameters from the semi-empirical crown fire rate of spread formula [62], or thresholds for transitioning to crown fire formulations. (Refer to Table 1 for specifics.) Aside from these varied parameters, the simulations used standard LANDFIRE surface and canopy fuel data for initialization. The simulations began using the second hour of a 36 h 13 km North American Mesoscale (NAM) weather forecast, starting at 11 AM on 8 September 2022 (18 UTC). At 2036 UTC on 8 September 2022, VIIRS active fire detection data of the ongoing fire were introduced at the model time of 37 min, and the CAWFE simulations continued throughout the remaining 34 h of the NAM forecast.

Table 1. Parameter settings for physics-varying CAWFE model ensemble members for Mosquito Fire.

	Fuel Factors (Amount and Moisture)			Factors Related to Wind Driving Fire			Model Smoothing		Crown Fire Parameters	
Ensemble Member	**% of Standard Surface Fuel Load and Depth**	**Dead Fuel Moisture Content and Diurnal Amplitude (%)**	**Canopy Fuel Moisture Content**	**Elevation to Which Winds Are Interpolated for Fire Spread**	**Vertical Grid Point Used for Winds**	**If Wind Speed < 0.5 m s^{-1}, Is ROS = 0?**	**Length Scale for Eddy Diffusion (d1–d3) and d4**	**Smoothing Coef. (VIS)**	**Crown Fire ROS Multiple of Surface Fire ROS**	**Threshold Flux for Transition to CF Based on HFGL (kW m^{-2})**
MQ01	100%	4.0 ± 0.2	90%	5 m AGL, log interp.	3	yes	180, 90	0.1	5	1.7
MQ02	50%	4.0 ± 0.2	90%	5 m AGL, log interp.	3	yes	180, 90	0.1	5	1.7
MQ03	200%	4.0 ± 0.2	90%	5 m AGL, log interp.	3	yes	180, 90	0.1	5	1.7
MQ04	100%	5.0 ± 0.2	90%	5 m AGL, log interp.	3	yes	180, 90	0.1	5	1.7
MQ05	100%	3.0 ± 0.2	90%	5 m AGL, log interp.	3	yes	180, 90	0.1	5	1.7
MQ06	100%	4.0 ± 0.2	90%	1.5 × fuel depth	3	yes	180, 90	0.1	5	1.7
MQ07	100%	4.0 ± 0.2	90%	5 m AGL, linear interp.	3	yes	180, 90	0.1	5	1.7
MQ08	100%	4.0 ± 0.2	90%	5 m AGL, linear interp.	2	yes	180, 90	0.1	5	1.7
MQ09	100%	4.0 ± 0.2	90%	5 m AGL, linear interp.	4	yes	180, 90	0.1	5	1.7
MQ10	100%	4.0 ± 0.2	90%	5 m AGL, log interp.	2	yes	180, 90	0.1	5	1.7
MQ11	100%	4.0 ± 0.2	90%	5 m AGL, log interp.	4	yes	180, 90	0.1	5	1.7
MQ12	100%	4.0 ± 0.2	90%	5 m AGL, log interp.	3	no	180, 90	0.1	5	1.7
MQ13	100%	4.0 ± 0.2	90%	5 m AGL, log interp.	3	yes	360,180	0.15	5	1.7
MQ14	100%	4.0 ± 0.2	90%	5 m AGL, log interp.	3	yes	180, 90	0.1	9	1.7
MQ15	100%	4.0 ± 0.2	90%	5 m AGL, log interp.	3	yes	180, 90	0.1	5	0.
MQ16	100%	4.0 ± 0.2	110%	5 m AGL, log interp.	3	yes	180, 90	0.1	5	1.7
MQ17	100%	4.0 ± 0.2	70%	5 m AGL, log interp.	3	yes	180, 90	0.1	5	1.7

3.4. SREF Weather Initialization of the Mosquito Fire and the Tubbs Fire

The third forecast hour of each SREF ensemble member was used to initialize a CAWFE simulation's atmospheric state. This data were also used to establish lateral boundary conditions at 3 h intervals through hour 39. CAWFE simulations were capped at a 36 h forecast because, beyond this point, the finer-resolution simulations tend to lose accuracy, typically retaining skill for only 1–2 days due to the inherent limits of atmospheric predictability. Regarding other CAWFE settings, ensemble members were initialized with LANDFIRE surface and canopy fuel data, along with a uniform set of physics parameters. This approach was applied to conduct ensemble simulations for two wildfires—the 2022 Mosquito Fire and the 2017 Tubbs Fire—during periods of active growth.

Ensemble members were configured with model settings consistent with MQ01 (refer to Table 1). The CAWFE simulations began at 11 AM on 8 September 2022 using data from the third hour of the 8 September 2022, 15 UTC SREF forecast. At 2036 UTC on 8 September 2022, VIIRS active fire detection data of the ongoing fire were integrated into the simulation at the model time of 2 h and 37 min and the simulation continued through 34 h.

The CAWFE ensemble simulation of the Tubbs Fire used model settings outlined in [67] but was initialized with the SREF ensemble members from the 8 October 2017, 1500 UTC forecast, with the ignition introduced as a point at 4 h 43 min into the simulation, and the simulation carried out for 14 h until the simulated fire exited the computational domain.

3.5. Fuel-Varying Initialization of the Caldor Fire

A fuel-varying CAWFE ensemble was applied to the Caldor Fire. From both the NAWFD fine woody debris (FWD) and aggregate tree fuel data strata, six fields of data were extracted: the mean, minimum, 25th percentile, 50th percentile, 75th percentile, and maximum values of the fuel load distribution for each existing vegetation type (as illustrated in Figure 4). These data points were used to replace surface fuel loads from LANDFIRE in each CAWFE ensemble member. Another member was initialized with standard surface fuel properties from the identified fuel model categorized using the Anderson 13 system and standard LANDFIRE canopy fuel loads (obtained by multiplying the canopy bulk density by the difference between the canopy height and the canopy base height).

All ensemble members were initialized using a NAM weather forecast, specifically, the second hour of the 16 August 2021, 18 UTC forecast, at 1 p.m. on 16 August 2021. Hourly boundary conditions were applied along with a surface fuel moisture content of 5%, subject to a 0.8% sinusoidal diurnal variability, and uniform physics settings. The fire was ignited in progress using the 16 August 2021, 2150 UTC VIIRS observation at 1 h and 50 min into the simulation, and the runs carried out for 23 h and 5 min.

The Caldor Fire represented an event driven both by moderate winds and energy released by the fire. It occurred in an area where fire mitigation by strategic fuel reduction was practiced. In fact, this period encompassed when the fire overran the community of Grizzly Flats, CA, where some but not all planned mitigation had occurred. Additional treatments were planned in areas approached by the fire in later periods. In addition, previous LiDAR measurements found substantial differences from common databases widely used for fire modeling. Thus, ensemble simulation of fire behavior examining differences due to fuel representation have additional significance for this area.

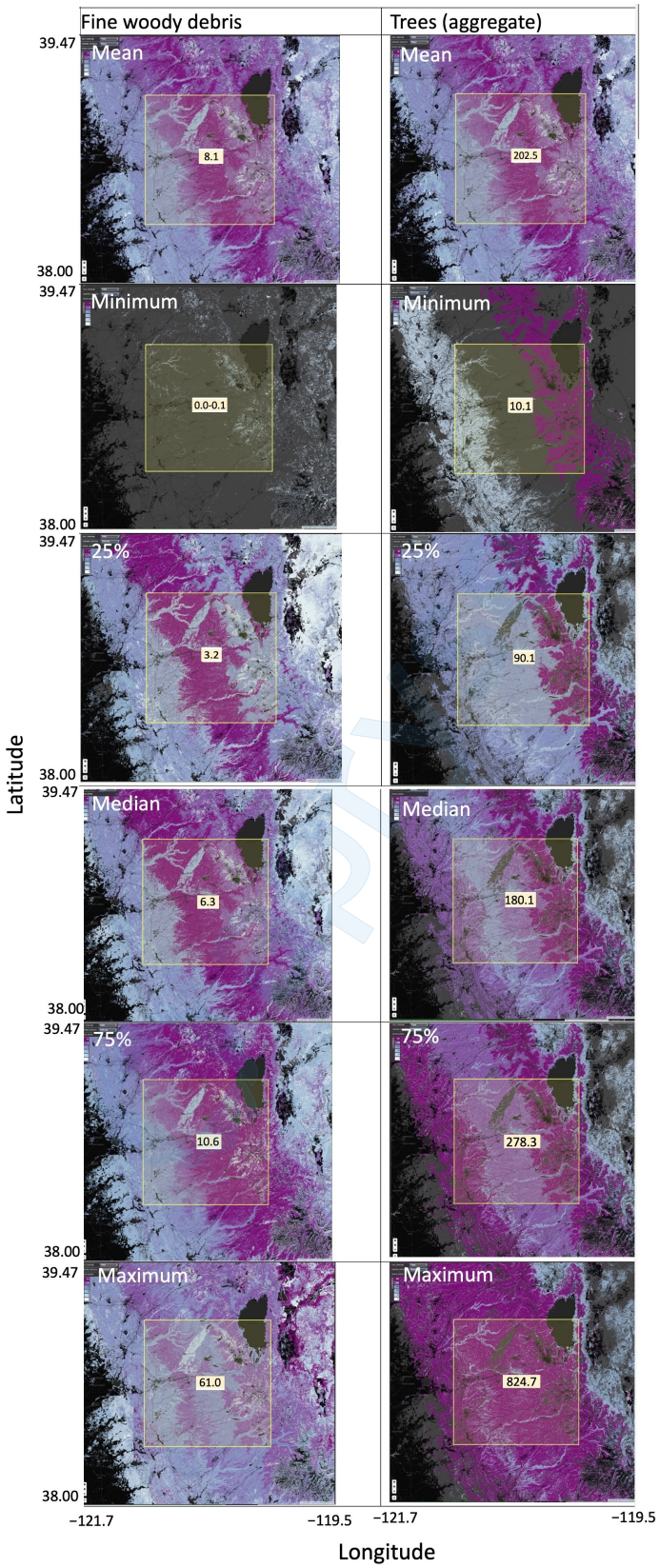

Figure 4. The (**left**) fine woody debris (surface) fuel loads and (**right**) aggregate tree (canopy) fuel loads associated with the existing vegetation types present in the vicinity of the Caldor Fire from the North American Wildland Fuels Database. Each entry's mean load for the rectangle sampled from (in Mg ha^{-1}) is given in the center box. Figures were generated using https://fuels.mtri.org.

4. Results

4.1. Simulation Results and Evaluation

This section presents the outcomes of several ensembles conducted to show how varying initialization approaches impact predicted uncertainty, as shown by variability among members. The ensembles use the CAWFE model, examining different initializations including SREF weather initialization, probabilistic fuel data initialization, and physics-varying ensemble forecasts. These are compared to observations from VIIRS. The objectives are to assess whether the ensemble prediction encapsulates the actual fire spread, to understand the influence of different initialization approaches on uncertainty, and to visualize the probabilistic outcomes.

4.1.1. Physics-Varying Ensemble Forecast of the Mosquito Fire

The 34 h simulation of the Mosquito Fire, conducted during a phase of plume-driven growth using a CAWFE ensemble with varied physics parameters (Table 1), produced modest differences among ensemble members (Figure 5). Variations in spread direction were minimal due to the dominant influence of river canyon topography, but discrepancies were noted in the spread rate along the northern and southeastern regions and into a bowl-shaped area on the fire's southern flank. The ensemble generally captured the outward expansion of the fire well compared to a VIIRS observation (Figure 6), although it missed a rapid growth to the southeast attributed to a sudden wind push from the northwest [74]. Outlier member MQ10, resulting from wind interpolation settings, successfully captured the rapid expansion but deviated by 45 degrees in direction and overestimated growth elsewhere. Collectively, the ensemble depicted both overall trends and an exceptional event in the fire's behavior.

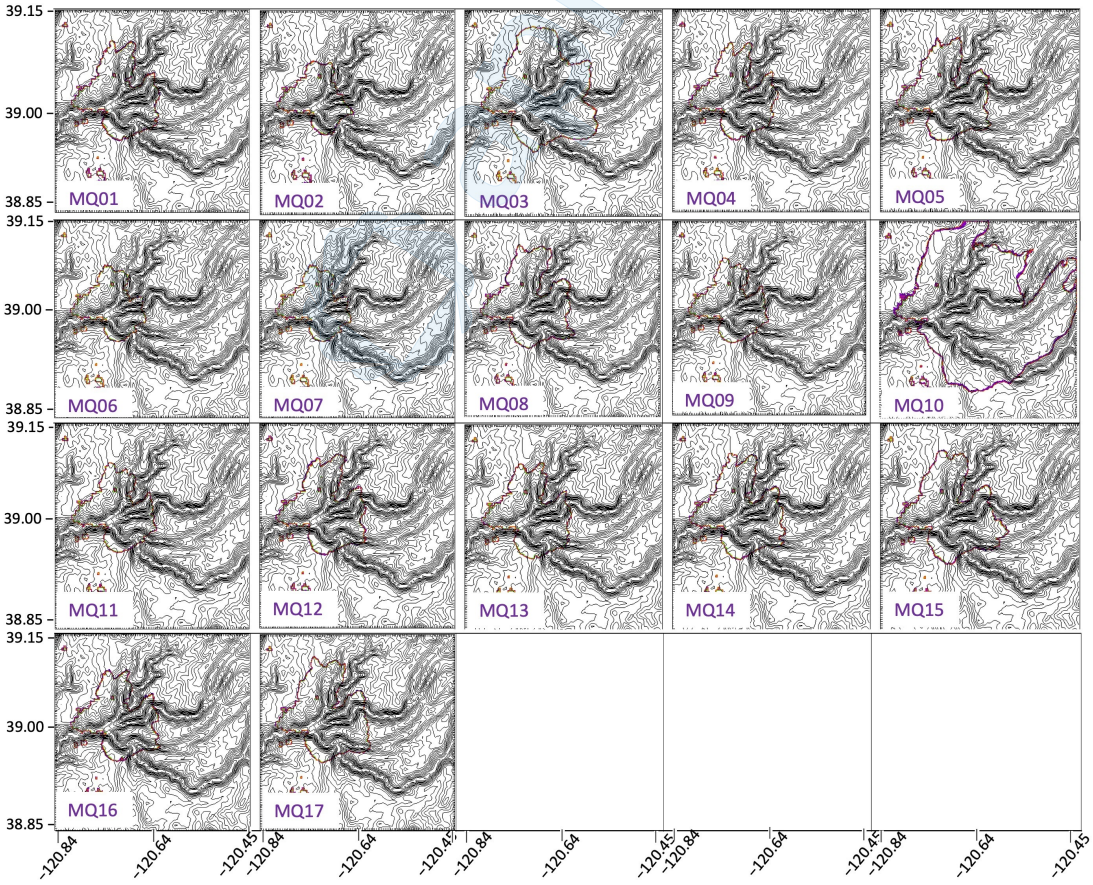

Figure 5. CAWFE ensemble members' simulations of the Mosquito Fire, highlighting the variation among simulations due to different physics parameters, as specified in Table 1. MQ01 was the control

experiment, around which other configurations were varied. The red contour outlines the simulated fire extent at the conclusion of the 34 h simulation, on 9 September 2022, at 11 p.m. local time. The terrain is shown with contour intervals of 54 m. The simulation domain covers an area of 33.3 km by 33.3 km.

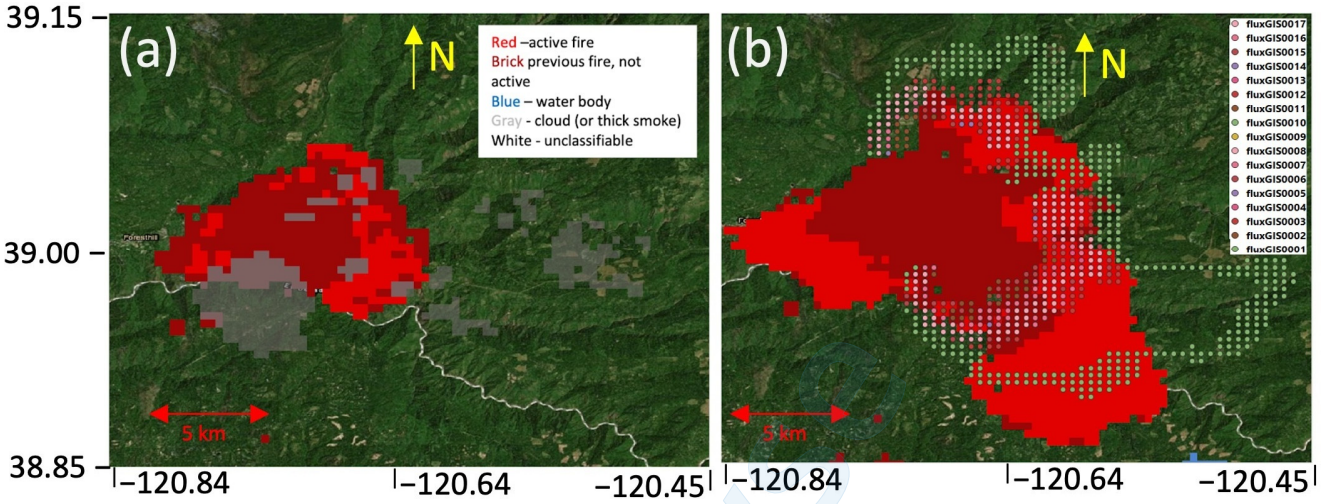

Figure 6. VIIRS images used to initialize and evaluate progression in simulations of the Mosquito Fire. Panel (**a**) shows the fire on 8 September 2022 at 2036 UTC and (**b**) displays the fire's state on 9 September 2022 at 1035 UTC, overlaid with ensemble member simulated fluxes at that time. The legend for satellite active fire detection data shown in (**a**) applies also to (**b**).

4.1.2. Short-Range Ensemble Forecast (SREF) Weather Initialization of the Mosquito Fire

A 26-member CAWFE ensemble, initialized with boundary conditions from each of the 26 SREF larger-scale weather forecasts, was run for the same 34 h period (Figure 7). The simulations exhibited little variability, clustering closely around the main body of the fire (Figure 8). More variability was observed among NMB members than ARW members, with differences primarily appearing in the last few NMB members (NP4–NP6), which predicted greater growth in the north-spreading region. No distinct outliers were produced, and all members missed the sudden southeast growth.

4.1.3. Short-Range Ensemble Forecast (SREF) Weather Initialization of the Tubbs Fire

Each CAWFE ensemble member began at 5 p.m. local time on 8 October 2017, using the ninth hour of the 15 UTC SREF forecast. The simulations varied in the spread rate of the leading edge, lateral expansion, and whether the fire veered toward the west later in the period (Figure 9). More variability was seen among NMB-initialized members than ARW-initialized members. Evaluation against the 9 October 2017, 1009 UTC VIIRS observation (Figure 10) showed that while the ensemble encompassed the observed fire perimeter, the predicted western veering by four members did not occur.

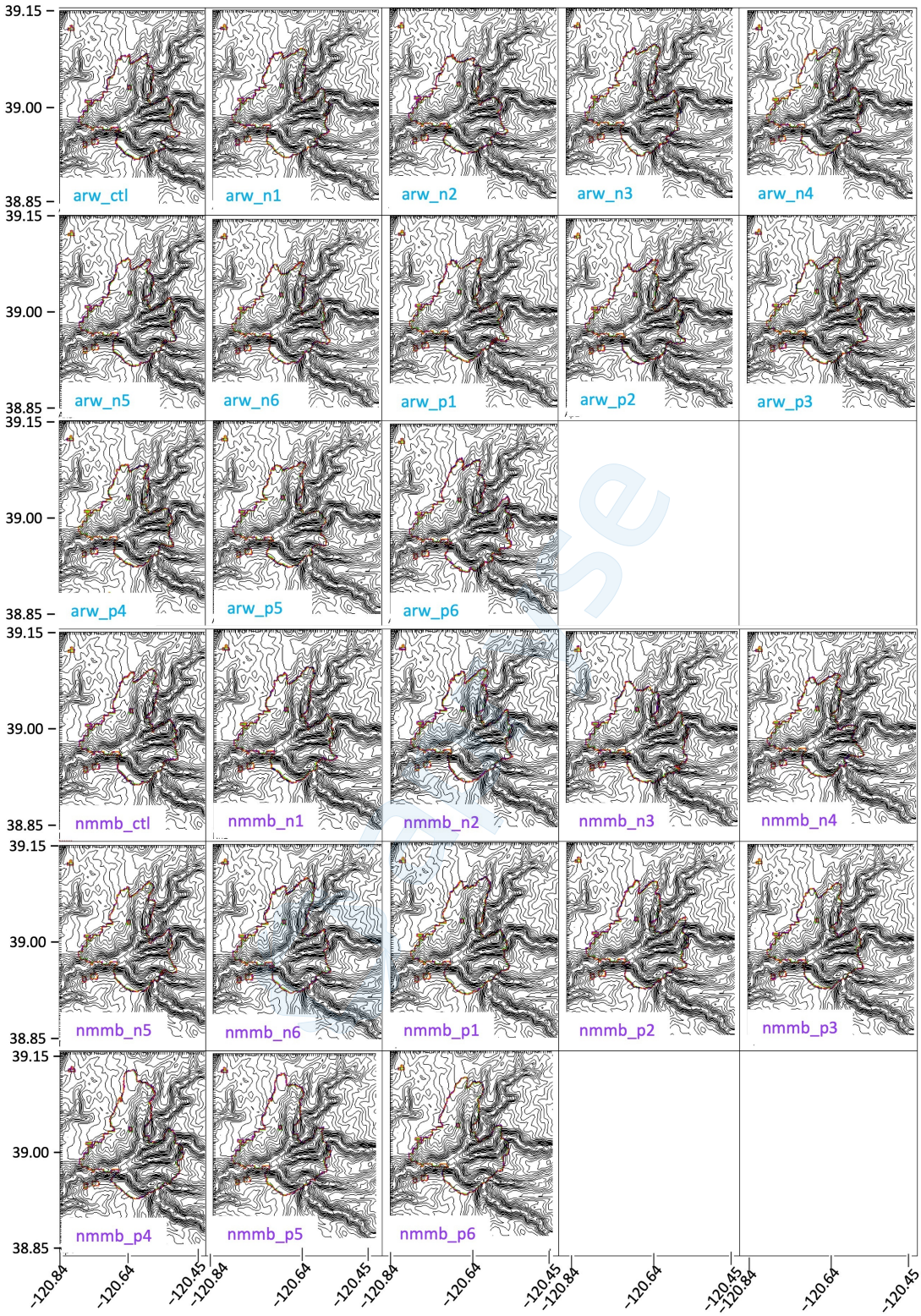

Figure 7. CAWFE ensemble members' simulations of the Mosquito Fire, each initialized by a different member of the Short-Range Ensemble Forecast (SREF) large-scale weather ensemble. The top 13 frames show simulations initialized by ARW-based members, while the bottom 13 frames show simulations initialized by NMB-based members. Each frame is labeled with the specific SREF member used for initialization. The red contour outlines the simulated fire extent at the end of the 34 h simulation period, on 9 September 2022, at 11 p.m. local time. Terrain contour intervals are 54 m, and the domain size is 33.3 km by 33.3 km.

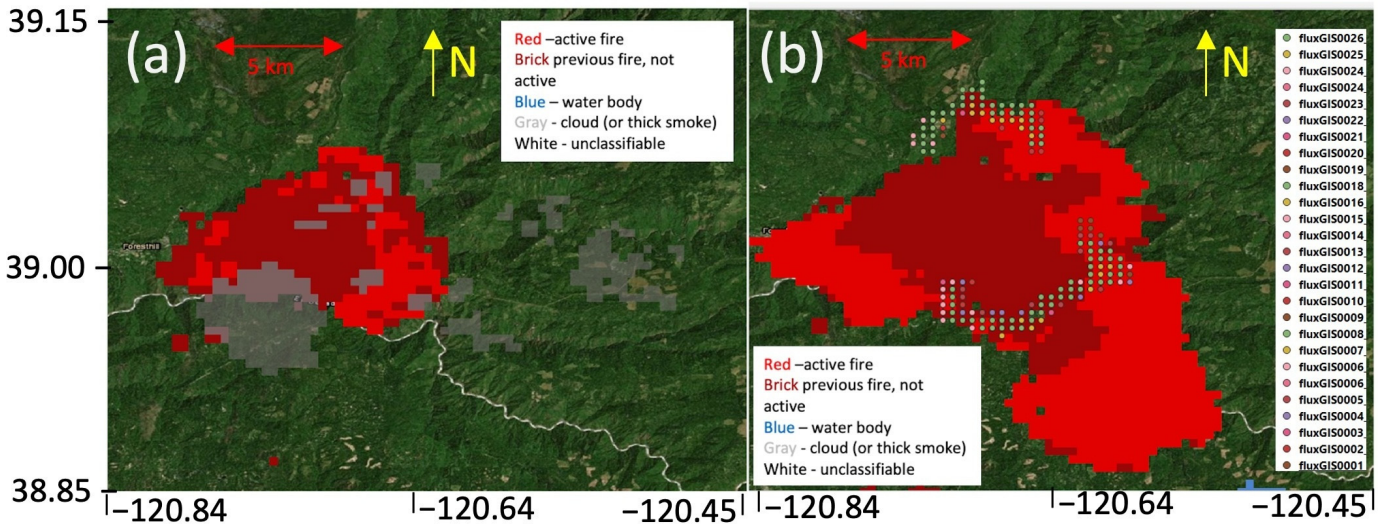

Figure 8. VIIRS data from the Mosquito Fire from (**a**) 8 September 2022, at 2036 UTC, the data used to initialize fire in progress, and (**b**) 9 September 2022, at 1035 UTC, over which lie ensemble member simulated fluxes initialized with 8 September 2022 15Z SREF members at that time.

4.1.4. Probabilistic Fuel Data Initialization of the Caldor Fire

An ensemble of CAWFE simulations, initialized with surface and canopy fuel loads statistically distributed around the mean loads for the mapped vegetation types, was compared to a simulation based on LANDFIRE fuel data (Figure 11). Despite wide-ranging fuel loads, simulations were remarkably similar, with only subtle increases in fire extent for increased surface fine woody debris or tree fuel loads. The LANDFIRE-based ensemble predicted more growth to the west. Compared to the VIIRS observation (Figure 12), the simulations encompassed the actual fire extent after 11.5 h of simulation, particularly the forward growth, but consistently overestimated bulging to the west.

4.2. Visualization Results

Graphic representations and communication methods were created to express the most likely outcomes for the spread of modeled solutions and occurrence of outliers. Three key probabilistic products were chosen: (1) burn probability (the likelihood of a given location on the landscape burning during the forecast period), (2) spread rate (the speed at which points on the fire line are moving), and (3) heat flux (a measure of the fire's intensity and a potential proxy for vegetative burn severity). These used model output variables commonly derivable in wildfire behavior modeling systems—(1) the time of arrival (TOA) of a modeled fire at a location, (2) instantaneous spread rate at points along the fire line (a key operational metric), and (3) minute by minute instantaneous output of the total sensible and latent heat flux from both surface and crown fires (a measure of energy released per unit area per unit time). Users desired both statistically combined ensemble outputs and the ability to inspect individual members to identify outliers. An example is given in Figure S1.

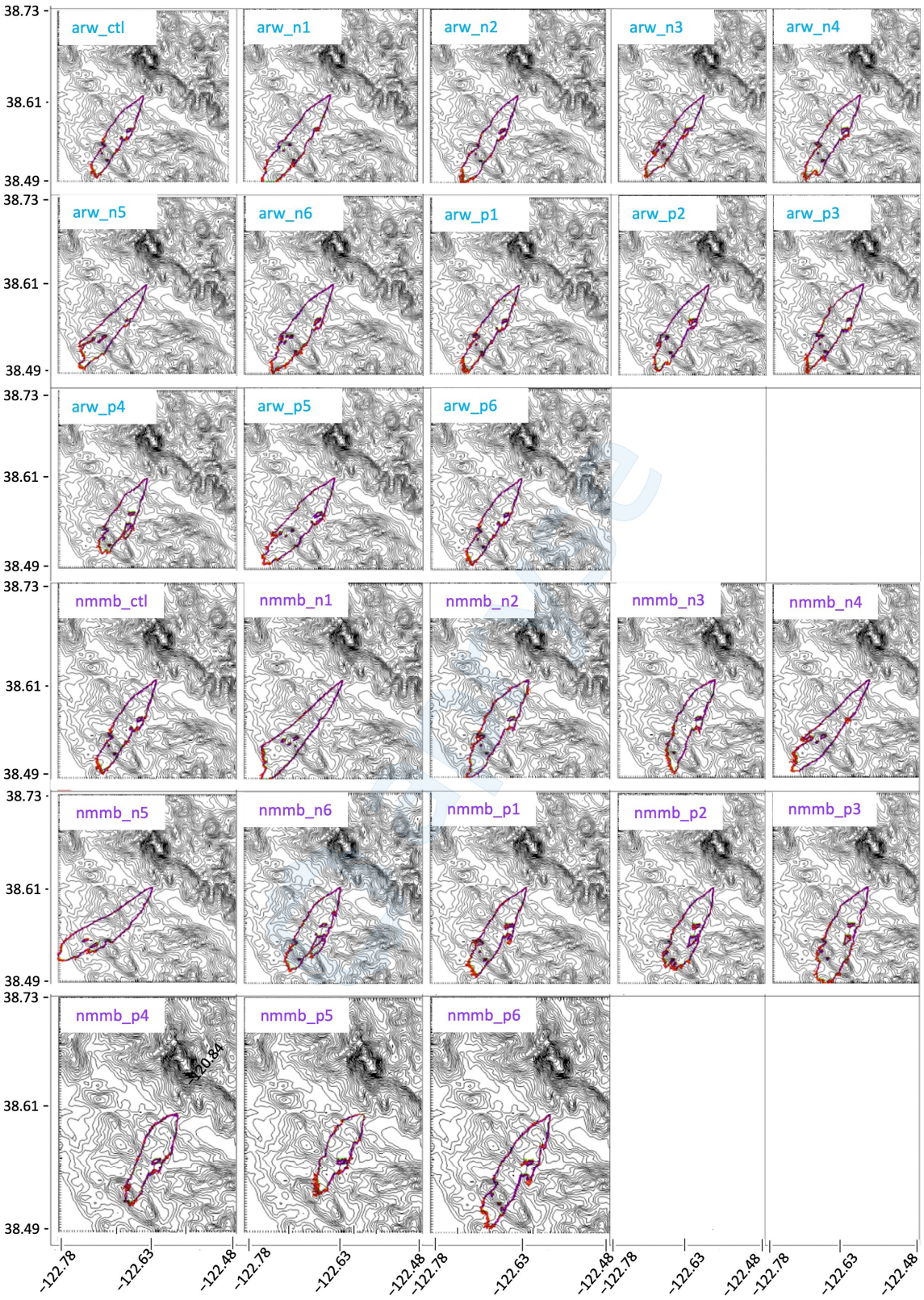

Figure 9. CAWFE ensemble simulations for the Tubbs Fire, initialized with varying SREF large-scale weather ensemble members. The top 13 frames represent ARW-based initializations, while the bottom 13 frames depict NMB-based initializations (details in text). The red contour delineates the simulated fire extent after 9 h of simulation, on 9 October 2017, at 4 a.m. local time. Terrain contours are shown at 31 m intervals in a domain spanning 26.7 km × 26.7 km.

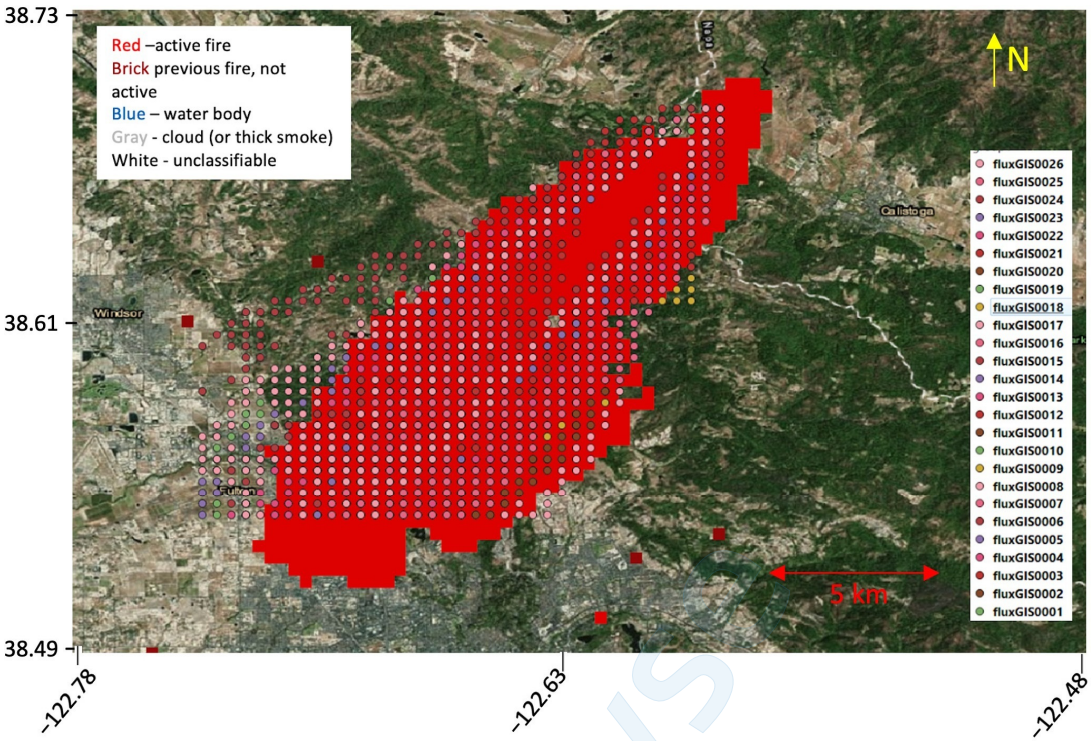

Figure 10. VIIRS data from the Tubbs Fire from 9 October 2017, at 1006 UTC (3:06 a.m. local time), over which lie ensemble member's simulated fluxes at that time. The Tubbs Fire CAWFE ensemble (the 26 members are coded by color in figure legend) was initialized from its ignition point at 0443 UTC (9:43 p.m. local time).

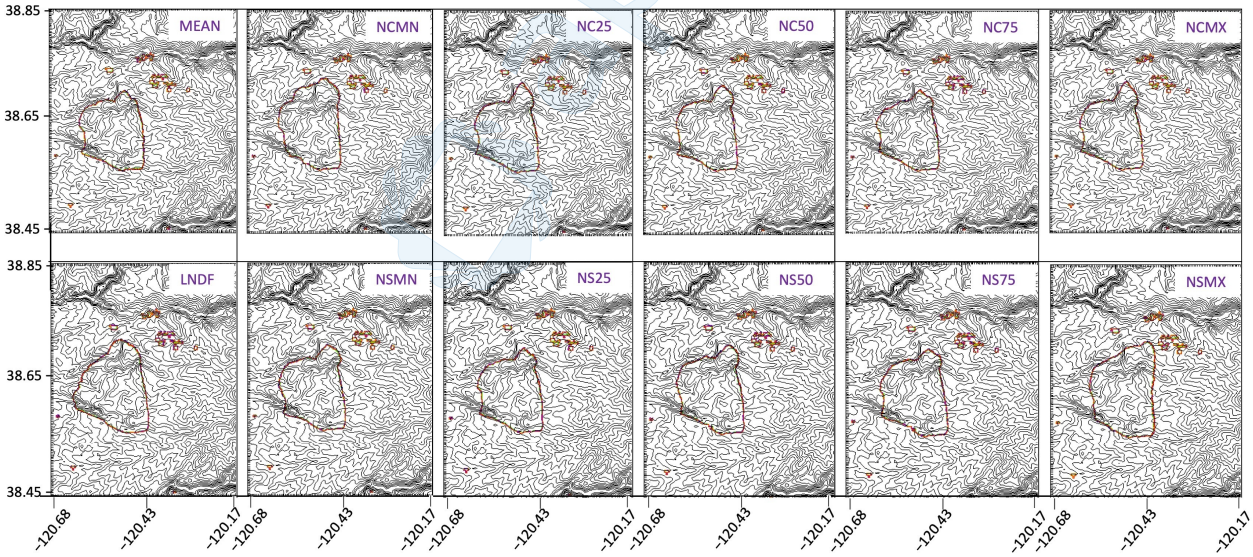

Figure 11. CAWFE ensemble members for simulations of the Caldor Fire, where each member is initialized with different fuel information, indicated in each frame. The top left figure uses mean NAWFD fire woody debris and tree fuel loads. The lower left figure is a simulation using the industry standard LANDFIRE fuel data. The top row uses mean fine woody debris fuel loads and (from left to right) minimum, 25th percentile, median, 75th percentile, and maximum tree fuel loads from NAWFD, respectively. The bottom row uses mean tree fuel loads and (from left to right) minimum, 25th percentile, median, 75th percentile, and maximum fine woody debris fuel loads, respectively. The red contour outlines the simulated fire extent after 23 h of simulation, on 17 August 2021, at 10 a.m. local time. Terrain contours are shown at 69 m intervals in a domain spanning 44.4 km × 44.4 km.

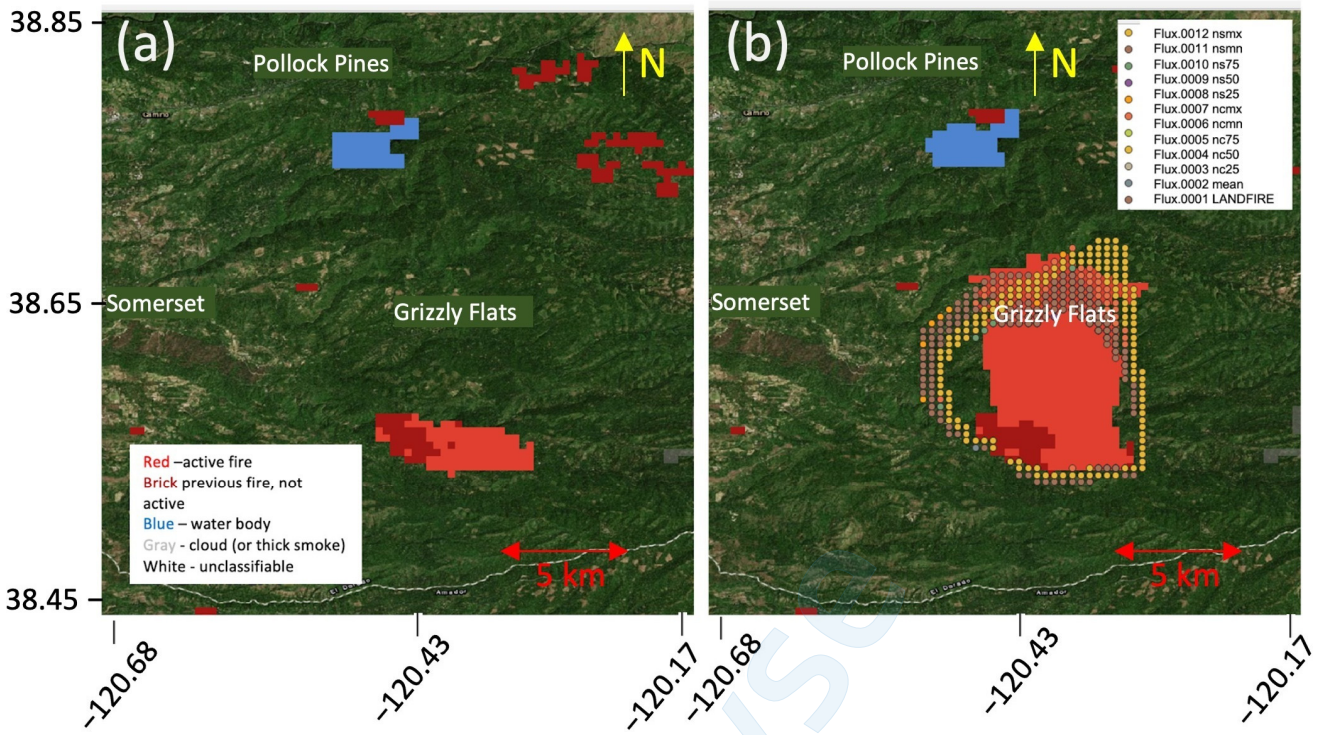

Figure 12. VIIRS data from the Caldor Fire from (**a**) 16 August 2021, at 2150 UTC (2:50 p.m. local time), the data used to initialize fire in progress, and (**b**) 17 August 2021, at 0919 UTC, (2:19 a.m. local time) over which lie ensemble member simulated fluxes at that time. The legend for satellite active fire detection data shown in (**a**) applies also to (**b**).

Burn probability was calculated by accumulating predicted fire tracks from ensemble members and calculating the percentage of members that overran each point within a spatial domain. Animating the burn probability provided a clearer expectation of evolving fire extent, as locations of uncertainty evolved over time. Presentation challenges included maintaining distinct delineation between contour steps while communicating chance quantity, spread direction, and advances in time. Outcomes for each ensemble included an animated layer showing the percentage of members that burned each cell by the hourly timestep (Figure 13a–d). The palette for burn probability met the highest federal and California AAA web accessibility standards, remaining distinct when overlaid on real-color Earth geographic imagery.

Spread rate indicates how fast the fire line is expanding and varies widely in time and space. One-minute interval outputs from the CAWFE model provide a 2-D map of instantaneous spread rate throughout the forecast period for each ensemble member. This detailed data allows for the visualization of spread rate values for all ensemble members during the fire's progression, identifying potential times and locations of rapid fire spread (Figure 14a). By plotting the standard deviation, areas of uncertainty are highlighted (Figure 14b). Additionally, the 95th percentile values for spread rate reveal potential locations of fire spread chutes (Figure 14c). The color schemes for these fields (Figure 14d) are chosen to meet the strictest web accessibility standards and maintain clarity when overlaid on typical maps and earth imagery. Expanding this graphical approach, an animation of the mean spread rate and standard deviation, such as in Video S2 of the SREF weather-varying ensemble for the Tubbs Fire, exposes areas where slight uncertainties in wind speed create local wind "hotspots" with higher uncertainty. In downslope wind events, where wind extrema are produced by certain combinations of near-surface wind speed, atmospheric static stability, and terrain aspect ratio, these locations can be associated with high-impact electric grid ignitions. This approach provides additional hazard information, possibly prompting increased scrutiny from managers or triggering additional in situ or remote observations.

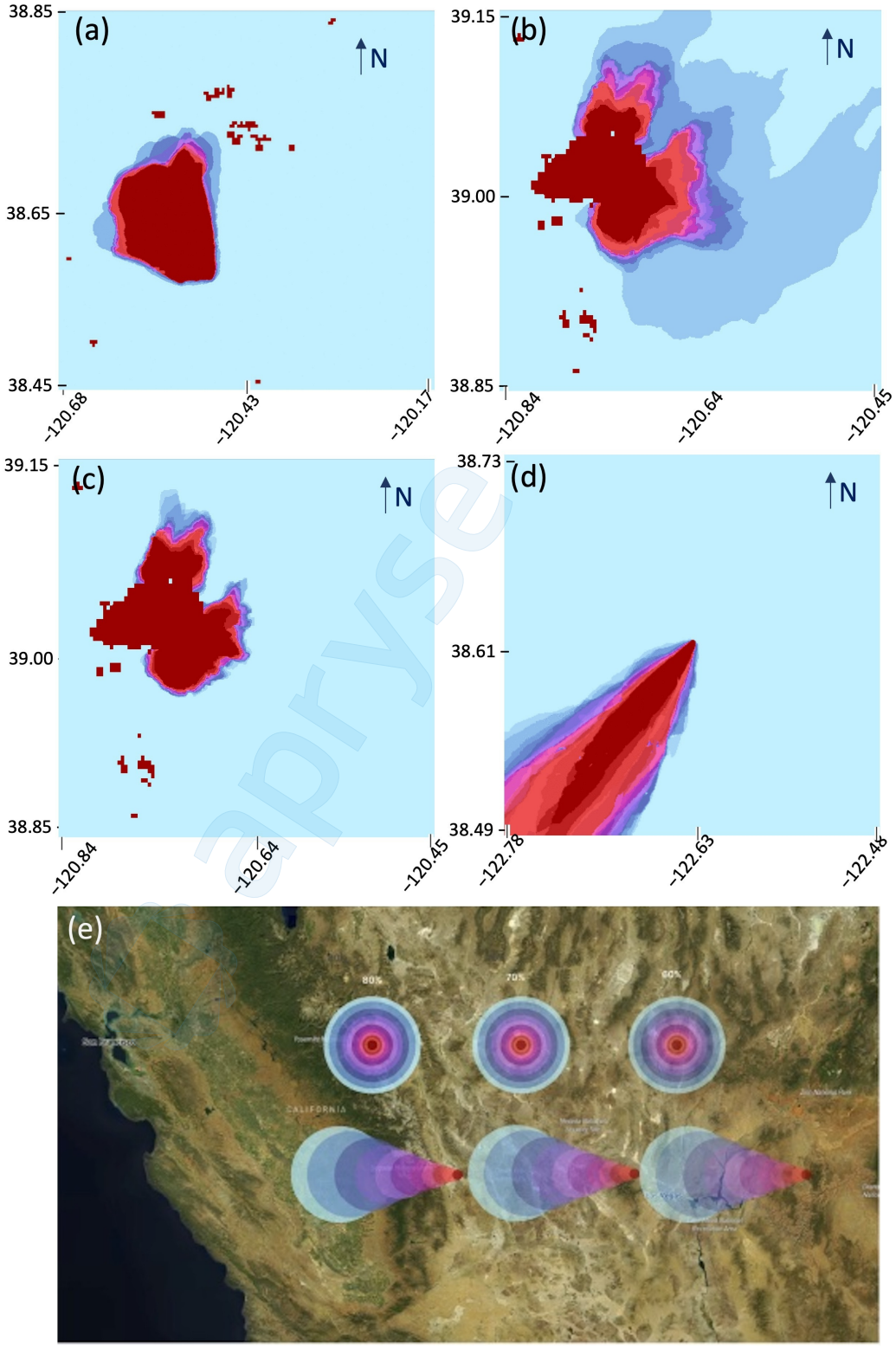

Figure 13. The burn probability (the percentage, 0–100%, in intervals of 10%) of ensemble members that burned each cell, shown at the end of the forecast period, for each ensemble: (**a**) Caldor Fire, (**b**) Mosquito Fire (physics-varying ensemble, (**c**) Mosquito Fire (SREF ensemble weather initialization), and (**d**) Tubbs Fire (SREF ensemble weather initialization). The color palette for (**a**–**d**) is shown in (**e**). This figure illustrates how burn probabilities were visualized, highlighting regions with varying likelihoods of burning based on ensemble forecasts.

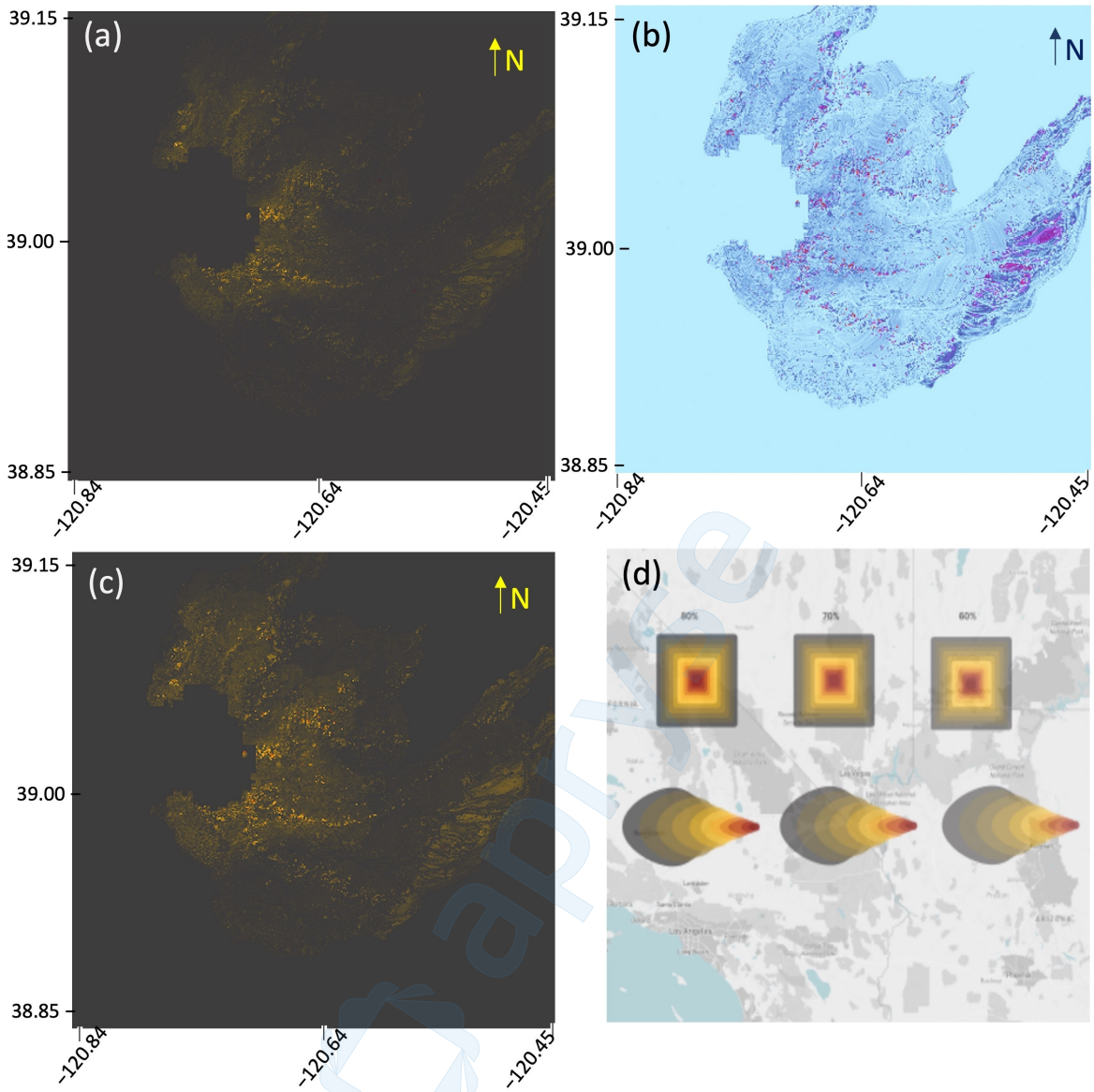

Figure 14. Montage of (**a**) mean spread rate, normalized to the maximum, identifying locations of rapid fire spread, and (**b**) standard deviation of the Mosquito Fire physics-varying ensemble, normalized to the maximum, at the end of the forecast period, indicating areas of uncertainty. (**c**) Layer shows the 95th percentile values for spread rate, normalized to the maximum, recorded within each cell at each timestep for the Mosquito Fire physics-varying ensemble, showing potential fire spread chutes. (**d**) The AAA compliance-rated color palette developed for spread rate, ensuring clarity and accessibility used in (**a**,**c**), where the range from 0.0 to 1.0 is divided into intervals of 0.1. Subfigure (**d**) shows three settings of transparency, which may be used as an additional accessibility tool. The standard deviation (**b**) uses the color palette shown in Figure 13e. This figure provides insights into the dynamics of fire spread and identifies regions of high uncertainty and potential rapid expansion.

Heat Flux, on its own, indicates where high intensity burning is occurring and, calculating either the maximum that occurred at a point as fire passed over it or the sum of energy released at a location, may reflect the degree of vegetation consumption (vegetative severity) and peak or cumulative impact to the soil properties, although in the latter, other soil factors need be considered. In physics-varying CAWFE ensembles of the Mosquito Fire, figures displayed mean total heat flux (Figure 15a) and variability (Figure 15b). The mean

total heat flux revealed intense burning and heat release, effectively serving as burning chutes, along the base of the river valleys through which the fire passed, as seen in traces of the highest values (i.e., the warmest colors, as shown in Figure 15c). The corresponding uncertainty plots (Figure 15b) showed the maximum uncertainty (hottest colors) lies in how far up the slopes of each river valley each member climbs—a good insight into the uncertain behavior of a plume-driven event.

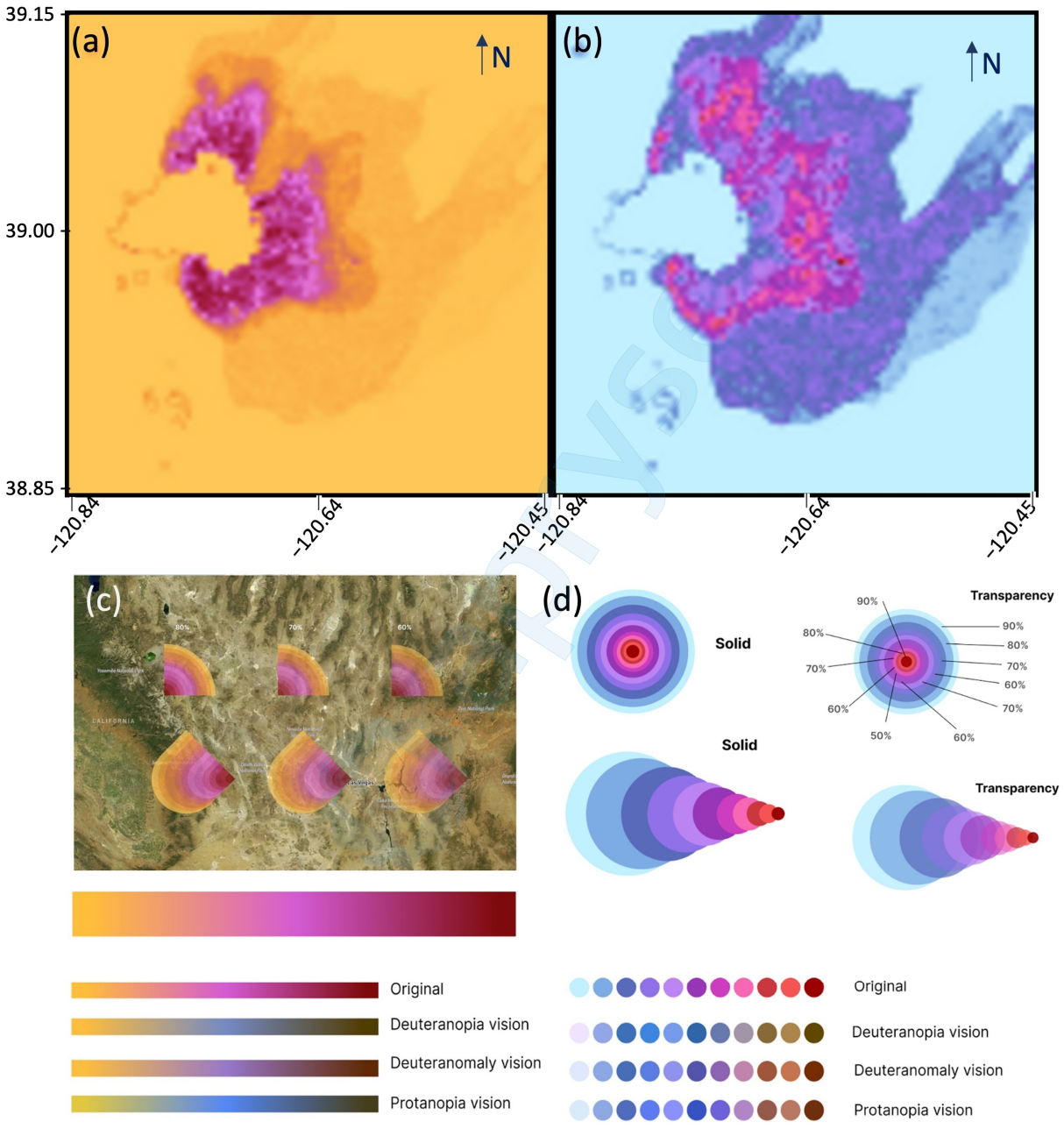

Figure 15. (**a**) The ensemble mean total (over the forecast) heat flux for the Mosquito Fire physics-varying ensemble, indicating locations of ensemble agreement on intense burning and heat release. (**b**) The standard deviation in heat flux, showing areas of uncertainty in the fire's behavior. The values in (**a**,**b**) range from 0.0 to 1.0, each normalized to the maximum, divided into intervals of 0.1. Color schemes selected for displaying heat flux mean, representing a temperature effect, and variability, showing how transparency can be used to maintain clarity and accessibility, are presented in (**c**,**d**), respectively.

Experiments varying the color ramps used to visualize heat flux mean and variability significantly affected their interpretation, drawing the eye to areas of disagreement among members. Heat flux invokes a sense of temperature, ranging from cold to hot, yet the commonly used colors in earth system science include reds and greens, which may be difficult to discern for people with color blindness. Our selection (Figure 15c) showcased clear differences in the mean value as they increased, akin to a straightforward temperature gradient. Clarity was upheld further when distinctions were conveyed through transparency (Figure 15d), as this secondary visual cue meets the 508 requirement and remains discernible when superimposed on real color earth imagery. Notably, the color scale is 508-compliant and is unambiguous for individuals with diverse red and green vision impairments (see Figure 15c,d).

5. Discussion

These initial attempts to apply uncertainty methods from numerical weather prediction to fire behavior forecasting yielded mixed results. In this work, some ensemble-forming approaches effectively portrayed a wide range of potential outcomes, including notable outliers, while others did not exhibit expected variability, even when applied to event types sensitive to specific environmental factors. Rather than evaluating the efficacy of a specific fire model, these findings provide insights and recommendations for future approaches to estimate uncertainty. This encompassing uncertainty framework holds promise for application across various fire models, though it is geographically limited due to the specific probabilistic fuel data and mesoscale ensemble weather forecasts used, which are tailored to the U.S.

Previous fire modeling works have used terms like "uncertainty" and "ensemble" but often in different contexts, sometimes equating uncertainty with model error. Unlike previous probabilistic studies [24,31,32,34–37] that employed kinematic fire models, our dynamic model approach could generate perturbations that amplify over time, distinguishing these results from prior work, where varying inputs showed model sensitivity to various factors rather than uncertainty. Our study revealed that while ensembles captured many unique characteristics of each wildfire event, the spread in burn probability was narrower than anticipated, particularly from varying key fire environment inputs of weather and fuel, indicating limited benefits from improving input data to reduce fire modeling errors. Other studies, such as [36], may have found different results due to varying inputs over implausibly wide ranges. The limited spread produced in these experiments from perturbed inputs yet wider variability in outcomes produced by varying physics parameters echoes the widely noted challenge of developing sufficient diversity among numerical weather prediction ensemble members [41]. However, limited spread among this work's ensemble members may have also occurred because, although nonlinear dynamics can produce rapidly diverging behavior, the forecast period in these simulations ranged from 12 to 34 h, perhaps too short to develop much divergence among members.

Probabilistic predictions, like deterministic forecasts, can be evaluated, but this must be done differently [41]; review, description, and evaluation of statistical evaluation methods was beyond the scope of this initial endeavor. Future efforts will focus on refining ensemble forecasting techniques, evaluating probabilistic predictions using appropriate statistical methods, and optimizing ensemble size to improve computational efficiency without compromising predictive accuracy. For instance, this investigation revealed that the weather-varying ensembles, each initialized with 13 members from two related weather models, could potentially be consolidated into a single 13-member ensemble using the NMMB model, leading to computational savings without limiting the diversity of outcomes.

Including multiple fire behavior and effects products in this work's probabilistic prediction outputs—such as spread rate and heat flux—provided additional scientific insights, identifying areas and times prone to uncertain fire behavior, such as in 'blow-ups' up valleys, chutes of intense burning, and occurrence of wind extrema in complex terrain. Additional physical insights arose from analysis of fuel-varying ensembles of the

Caldor Fire, which suggested that widespread landscape-scale fuel reduction may have had limited impacts on fire behavior during its run through the Grizzly Flats community, although more impactful effects of mitigation could occur beneath the scales resolved by these simulations.

Statistical reduction of this work's ensemble outputs to companion mean and variability plots brought out features upon which ensemble members agreed (e.g., areas where the fire will spread rapidly or burn intensely) as well as indicating locations of uncertainty (e.g., how widely a fire may swerve). A practical outcome from this methodology may be that times and/or locations of increased uncertainty or outlier behavior may be revealed, indicating a need for increased manager attention or more targeted observations. For example, these might predict wind "hotspots", potential electric grid disruptions, and heightened probability of wildfire ignitions. Scientific visualization of ensemble predictions has rapidly advanced and increased in sophistication. In this work, information interpretability was increased first by simply animating combined ensemble products, compared to the static burn probability presentation common in this field because uncertainty varies in time as well as space. Secondly, offering animations of individual members satisfies the need to inspect particular members or outliers. Additional statistical sectioning (such as distilling the top few percent or quartiles) was conducted and may have specific uses.

The shift towards internet-delivered information and the need for web accessibility compliance have underscored the need for improved methods to communicate uncertainty in fire predictions. In this study, surprisingly important but to-date underemphasized aspects of presenting probabilistic information emerged by including a graphic designer's input. Fire prediction information has historically been presented in hot–cold color palettes that can exclude users with a range of vision impairments. This work developed intuitive color palettes for each type of information and created presentation modes that showed clear demarcation between intervals, integrated more than one method for showing gradations (e.g., color and transparency), and satisfied the highest levels of web accessibility—a necessity for products serving federal and many state users.

6. Conclusions

This work's findings challenged the assumption that reducing uncertainty inherently diminishes error in fire behavior modeling. Despite a broad spectrum of inputs, the range of predicted outcomes remained constrained over forecast periods, highlighting the inherent limitations of solely improving input data to rectify model deficiencies. Varying physics parameters, however, created wider spreads in burn probability predictions, emphasizing the need to address gaps in fire process modeling knowledge.

Statistical reduction of ensembles to mean and variability plots revealed areas of agreement among ensemble members regarding rapid fire spread or intense burning, while also pinpointing locations of uncertainty regarding fire behavior. This study also emphasized the importance of enhancing information interpretability, even through simple innovations such as animations of both ensemble and individual ensemble member products and the development of intuitive color palettes for presenting probabilistic information. These enhancements aimed to improve accessibility and clarity in fire prediction outputs, addressing historical limitations in visual presentation methods.

Looking ahead, future directions for research include refinements in ensemble forecasting techniques, development of robust statistical methods for evaluating probabilistic predictions, and optimizing ensemble size to achieve computational efficiency without compromising predictive accuracy. Recent advancements in ensemble visualization techniques have set a precedent for more sophisticated and informative presentations of fire behavior predictions. The methods developed here not only improve the accessibility and interpretability of fire forecast data but also enable stakeholders to better grasp the range of uncertainties associated with fire behavior. These efforts could further advance the field of fire behavior forecasting and enhance its value in operational and management applications.

Supplementary Materials: The following supporting information can be downloaded at: https://www.mdpi.com/article/10.3390/fire7070227/s1, Figure S1: Time of arrival (in tenths of simulation duration, from cool (blue) to hot (red) in CAWFE ensemble individual members, for simulations of the Mosquito Fire, where the parameters governing each member are given in Table 1; Video S2: Animated montage of (a) mean spread rate and (b) standard deviation for the Tubbs Fire initialized with the SREF weather-varying ensemble. In downslope wind events, wind extrema sometimes associated with electric grid ignitions are produced by certain combinations of near surface wind speed, atmospheric static stability, and terrain aspect ratio. The graphical approach in this figure indicates areas where slight uncertainties in the wind speed led to local wind "hotspots".

Author Contributions: Conceptualization, J.L.C., G.W.J., J.S.R. and D.S.; methodology, J.L.C., J.S.R., G.W.J. and D.S.; software, J.L.C. and G.W.J.; validation, J.L.C., J.S.R. and D.S.; formal analysis, J.L.C. and G.W.J.; investigation, J.L.C., J.S.R. and G.W.J.; resources, J.S.R. and D.S.; data curation, J.L.C. and G.W.J.; writing—original draft preparation, J.L.C. and J.S.R.; writing—review and editing, J.S.R., G.W.J. and D.S.; visualization, J.L.C. and G.W.J.; supervision, D.S.; project administration, J.S.R.; funding acquisition, J.L.C., G.W.J., J.S.R. and D.S. All authors have read and agreed to the published version of the manuscript.

Funding: This material is based upon work supported by the USDA NIFA Award #2022-33530-3727; the National Science Foundation under Awards 2038759 and 2209994; NIST under award 70NANB19H054; California Energy Commission, Comprehensive Open Source Development of Next Generation Wildfire Models for Grid Resiliency EPC-18-026, and NASA under Awards 80NSSC20K0206 and 80NSSC23K1393. NSF NCAR is sponsored by the U.S. National Science Foundation.

Institutional Review Board Statement: Not applicable.

Informed Consent Statement: Not applicable.

Data Availability Statement: CAWFE and other materials are available by request from J.L.C. No new data were created in this study.

Acknowledgments: We thank C. Andrea Raschke for contributing graphical design expertise; Craig Schwartz and Judith Berner for generously sharing their expertise and guidance on ensemble forecasting techniques; and Chris Johnson for invaluable guidance in identifying relevant references on visualization. Their insights greatly improved this work's content.

Conflicts of Interest: The authors declare no conflicts of interest.

References

1. Oldham, J. Wildfires in Colorado are Growing More Unpredictable. Officials Have Ignored the Warnings. ProPublica. 27 December 2022. Available online: https://www.propublica.org/article/colorado-marshall-fire-wildfire-climate-change (accessed on 20 June 2024).
2. Fernandes, P.M.; Botelho, H.S. A review of prescribed burning effectiveness in fire hazard reduction. *Int. J. Wildland Fire* **2008**, *12*, 117–128. [CrossRef]
3. Brodie, E.G.; Knapp, E.E.; Brooks, W.R.; Drury, S.A.; Ritchie, M.W. Forest thinning and prescribed burning treatments reduce wildfire severity and buffer the impacts of severe fire weather. *Fire Ecol.* **2024**, *20*, 17. [CrossRef]
4. National Academies of Science, Engineering, and Medicine. *Wildland Fires: Toward Improved Understanding and Forecasting of Air Quality Impacts: Proceedings of a Workshop*; The National Academies Press: Washington, DC, USA, 2022; p. 80. [CrossRef]
5. National Wildfire Coordinating Group. NWCG Standards for Prescribed Fire Planning and Implementation. May 2022. PMS 484. 47p. Available online: https://fs-prod-nwcg.s3.us-gov-west-1.amazonaws.com/s3fs-public/publication/pms484.pdf?VersionId=oC9h8HojgmacXiXrC9WFYZy3KNZwh84X (accessed on 24 April 2024).
6. Coen, J.L.; Schroeder, W.; Conway, S.; Tarnay, L. Computational modeling of extreme wildland fire events: A synthesis of scientific understanding with applications to forecasting, land management, and firefighter safety. *J. Comput. Sci.* **2020**, *45*, 101152. [CrossRef]
7. Johnson, M.M.; Garcia- Menendez, F. A comparison of smoke modelling tools used to mitigate air quality impacts from prescribed burning. *Int. J. Wildland Fire* **2023**, *32*, 1162–1173. [CrossRef]
8. Page, W.G.; Freeborn, P.H.; Butler, B.W.; Jolly, W.M. A review of US wildland firefighter entrapments: Trends, important environmental factors and research needs. *Int. J. Wildland Fire* **2019**, *28*, 551–569. [CrossRef]
9. Finney, M.A.; McAllister, S.S.; Grumstrup, T.P.; Forthofer, J.M. *Wildland Fire Behaviour: Dynamics, Principles and Processes*; CSIRO Publishing: Melbourne, Australian, 2021; p. 359.
10. Finney, M.A. *FARSITE: Fire Area Simulator—Model Development and Evaluation*; US Forest Service, Rocky Mountain Research Station: Ogden, UT, USA, 2004; Research Paper RMRS-RP-4 Revised; p. 52.

11. Finney, M.A. Fire growth using minimum travel time methods. *Can. J. For. Res.* **2002**, *32*, 1420–1424. [CrossRef]
12. Noonan-Wright, E.K.; Opperman, T.S.; Finney, M.A.; Zimmerman, G.T.; Seli, R.C.; Elenz, L.M.; Calkin, D.E.; Fiedler, J.R. 2011: Developing the US Wildland Fire Decision Support System. *J. Combust.* **2011**, *168473*, 14. [CrossRef]
13. Cardil, A.; Monedero, S.; SeLegue, P.; Navarrete, M.A.; de-Miguel, S.; Purdy, S.; Marshall, G.; Chavez, T.; Allison, K.; Quilez, R.; et al. Performance of operational fire spread models in California. *Int. J. Wildland Fire* **2023**, *32*, 1492–1502. [CrossRef]
14. University of California San Diego. WIFIRE. Available online: https://wifire.ucsd.edu (accessed on 20 April 2024).
15. Lautenberger, C. Wildland Fire Modeling with an Eulerian Level Set Method and Automated Calibration. *Fire Saf. J.* **2013**, *62*, 289–298. [CrossRef]
16. Johnson, G.W. (Spatial Informatics Group, Pleasanton, CA, USA); Saah, D. (Spatial Informatics Group, Pleasanton, CA, USA); Moritz, M. (Spatial Informatics Group, Pleasanton, CA, USA); Cheung, K. (Spatial Informatics Group, Pleasanton, CA, USA). The GridFire Fire Behavior Model. 2022; Unpublished work.
17. Coen, J.L. *Modeling Wildland Fires: A Description of the Coupled Atmosphere-Wildland Fire Environment Model (CAWFE)*; NCAR Technical Note NCAR/TN-500+STR; NCAR: Boulder, CO, USA, 2013.
18. Coen, J.L.; Cameron, M.; Michalakes, J.; Patton, E.G.; Riggan, P.J.; Yedinak, K.M. WRF-Fire: Coupled Weather-Wildland Fire Modeling with the Weather Research and Forecasting Model. *J. Appl. Meteor. Climatol.* **2013**, *52*, 16–38. Available online: http://journals.ametsoc.org/doi/pdf/10.1175/JAMC-D-12-023.1 (accessed on 20 June 2024). [CrossRef]
19. Linn, R.R. A Transport Model for Prediction of Wildfire Behavior. Ph.D. Thesis, New Mexico State University, Las Cruces, NM, USA, 1997.
20. Mell, W.E.; Jenkins, M.A.; Gould, J.S.; Cheney, N.P. A physics-based approach to modeling grassland fires. *Int. J. Wildland Fire* **2007**, *16*, 1–22. [CrossRef]
21. Vanella, M.; McGrattan, K.; McDermott, R.; Forney, G.; Mell, W.; Gissi, E.; Fiorucci, P. A multi-fidelity framework for wildland fire behavior simulations over complex terrain. *Atmosphere* **2021**, *12*, 273. [CrossRef]
22. Linn, R.R.; Goodrick, S.L.; Brambilla, S.; Brown, M.J.; Middleton, R.S.; O'Brien, J.J.; Hiers, J.K. QUIC-fire: A fast-running simulation tool for prescribed fire planning. *Environ. Model. Softw.* **2020**, *125*, 104616. [CrossRef]
23. Jimenez, E.; Hussaini, M.Y.; Goodrick, S. Quantifying parametric uncertainty in the Rothermel model. *Int. J. Wildland Fire* **2008**, *17*, 638–649. [CrossRef]
24. U.S.D.A. Forest Service. WFDSS Reference Guide Overview FSPro 1.0. Available online: https://wfdss.usgs.gov/wfdss/pdfs/fspro_reference.pdf (accessed on 20 April 2024).
25. Gigerenzer, G.; Hertwig, R.; van den Boeck, E.; Fasalo, B.; Katsikopoulos, K.V. "A 30% chance of rain tomorrow": How does the public understand probabilistic weather forecasts? *Risk Anal.* **2005**, *25*, 623–629. [CrossRef] [PubMed]
26. Doswell, C.; Brooks, H. Probabilistic Forecasting—A Primer. Available online: https://www.nssl.noaa.gov/users/brooks/public_html/prob/Probability.html (accessed on 20 April 2024).
27. Taleb, N. *The Black Swan: The Impact of the Highly Improbable*; Random House: New York, NY, USA, 2007; p. 400.
28. Lareau, N.P.; Nauslar, N.J.; Abatzoglou, J.T. The Carr fire vortex: A case of pyrotornadogenesis? *Geophys. Res. Lett.* **2018**, *45*, 13–107. [CrossRef]
29. Coen, J.L. *Simulation and analysis of the 2018 Carr Fire*; NSF NCAR: Boulder, CO, USA, 2023; *to be submitted*.
30. McLauchlan, K.; Higuera, P.; Miesel, J.R.; Rogers, B.; Schweitzer, J.; Shuman, J.; Tepley, A.; Varner, J.; Veblen, T.; Adalsteinsson, S.; et al. Fire as a fundamental ecological process: Research advances and frontiers. *J. Ecol.* **2020**, *108*, 2047–2069. [CrossRef]
31. Cruz, M.G. Monte Carlo-based ensemble method for prediction of grassland fire spread. *Int. J. Wildland Fire* **2010**, *19*, 521–530. [CrossRef]
32. Penman, T.D.; Ababei, D.A.; Cawson, J.G.; Cirulis, B.A.; Duff, T.J.; Swedosh, W.; Hilton, J.E. Effect of weather forecast errors on fire growth model projections. *Int. J. Wildland Fire* **2020**, *29*, 983–994. [CrossRef]
33. Toth, Z.; Kalnay, E. Ensemble forecasting at NMC: The generation of perturbations. *Bull. Am. Meteorol. Soc.* **1993**, *74*, 2317–2330. [CrossRef]
34. Finney, M.A.; Grenfell, I.C.; McHugh, C.W.; Seli, R.C.; Trethewey, D.; Stratton, R.D.; Brittain, S. A Method for Ensemble Wildland Fire Simulation. *Environ. Model. Assess.* **2011**, *16*, 153–167. [CrossRef]
35. Pinto, R.M.S.; Benali, A.; Sá, A.C.L.; Fernandes, P.M.; Soares, P.M.M.; Cardoso, R.M.; Trigo, R.M.; Pereira, J.M.C. Probabilistic fire spread forecast as a management tool in an operational setting. *SpringerPlus* **2016**, *5*, 1205. [CrossRef] [PubMed]
36. Benali, A.; Ervilha, A.R.; Sa, A.C.L.; Fernandes, P.M.; Pinto, R.M.S.; Trigo, R.M.; Pereira, J.M.C. Deciphering the impact of uncertainty on the accuracy of large wildfire spread simulations. *Sci. Total Environ.* **2016**, *569–570*, 73–85. [CrossRef] [PubMed]
37. Allaire, F.; Filippi, J.-B.; Mallet, V. Generation and evaluation of an ensemble of wildland fire simulations. *Int. J. Wildland Fire* **2016**, *29*, 160–173. [CrossRef]
38. Betz, J. What Is 508 Compliance (+Does It Apply to You)? Available online: https://www.g2.com/articles/508-compliance (accessed on 20 April 2024).
39. World Meteorological Organization. Guidelines on Ensemble Prediction Systems and Forecasting. *WMO-No. 1091*. 2012. Available online: https://library.wmo.int/pmb_ged/wmo_1091_en.pdf (accessed on 20 April 2024).
40. Murphy, A.H. What is a good forecast? An essay on the nature of goodness in weather forecasting. *Wea. Forecast.* **1993**, *8*, 281–293. [CrossRef]

41. Du, J.; Berner, J.; Buizza, R.; Charron, M.; Houtekamer, P.; Hou, D.; Jankov, I.; Mu, M.; Wang, X.; Wei, M.; et al. Ensemble Methods for Meteorological Predictions. In *Handbook of Hydrometeorological Ensemble Forecasting*; Duan, Q., Pappenberger, F., Wood, A., Cloke, H., Schaake, J., Eds.; Springer: Berlin/Heidelberg, Germany, 2019; pp. 99–149. [CrossRef]
42. NCEP Short-Range Ensemble Forecast (SREF). Available online: https://www.emc.ncep.noaa.gov/emc/pages/numerical_forecast_systems/sref.php (accessed on 20 April 2024).
43. National Oceanic and Atmospheric Administration, NCEP SREF 3-Hourly Forecast. Available online: https://www.spc.noaa.gov/exper/sref/srefplumes/ (accessed on 20 April 2024).
44. Anderson, H.E. Aids to determining fuel models for estimating fire behavior. In *General Technical Report INT-122*; USDA Forest Service, Intermountain Forest and Range Experiment Station: Ogden, UT, USA, 1982.
45. Scott, J.H.; Burgan, R.E. *Standard Fire Behavior Fuel Models: A Comprehensive Set for Use with Rothermel's Surface Fire Spread Model*; Gen. Tech. Rep. RMRS-GTR-153; U.S. Department of Agriculture, Forest Service, Rocky Mountain Research Station: Fort Collins, CO, USA, 2005. Available online: https://www.fs.usda.gov/rm/pubs/rmrs_gtr153.pdf (accessed on 26 June 2024).
46. Kennedy, M.C.; Prichard, S.J.; McKenzie, D.; French, N.H.F. Quantifying how sources of uncertainty in combustible biomass propagate to prediction of wildland fire emissions. *Int. J. Wildland Fire* **2020**, *29*, 793–806. [CrossRef]
47. Prichard, S.J.; Kennedy, M.C.; Andreu, A.G.; Eagle, P.C.; French, N.H.; Billmire, M. Next-generation biomass mapping for regional emissions and carbon inventories: Incorporating uncertainty in wildland fuel characterization. *J. Geophys. Res. Biogeosci.* **2019**, *124*, 3699–3716. [CrossRef]
48. Xu, Q.; Man, A.; Fredrickson, M.; Hou, Z.; Pitkanen, J.; Wing, B.; Ramirez, C.; Li, B.; Greenberg, J.A. Quantification of uncertainty in aboveground biomass estimates derived from small-footprint airborne LiDAR. *Remote Sens. Environ.* **2018**, *216*, 514–528. [CrossRef]
49. California Forest Observatory. Available online: https://forestobservatory.com (accessed on 20 April 2024).
50. Popescu, S.C.; Zhao, K. A voxel-based lidar method for estimating crown base height for deciduous and pine trees. *Remote Sens. Environ.* **2008**, *112*, 767–781. [CrossRef]
51. Coen, J.L.; Stavros, E.N.; Fites-Kaufman, J.A. Deconstructing the King megafire. *Ecol. Appl.* **2018**, *28*, 1565–1580. Available online: https://esajournals.onlinelibrary.wiley.com/doi/10.1002/eap.1752 (accessed on 20 April 2024). [CrossRef]
52. Tarnay, T.; Conway, S.; Coen, J. The Use of Remote Sensing and Coupled Weather-Fire Modeling for Hazard Identification And Testing Mitigation Impacts in The Northern Sierra Nevada Mountains. In Proceedings of the Fire Continuum Conference, Missoula, MT, USA, 21–24 May 2018.
53. Wang, J.; Hazarika, S.; Li, C.; Shen, H.-W. Visualization and Visual Analysis of Ensemble Data: A Survey. *IEEE Trans. Vis. Comput. Graph.* **2019**, *25*, 2853–2872. [CrossRef] [PubMed]
54. Kumpf, A.; Tost, B.; Baumgart, M.; Riemer, M.; Westermann, R.; Rautenhaus, M. Visualizing confidence in cluster-based ensemble weather forecast analyses. *IEEE Trans. Vis. Comput. Graph.* **2018**, *24*, 109–119. [CrossRef] [PubMed]
55. Ferstl, F.; Burger, K.; Westermann, R. Streamline variability plots for characterizing the uncertainty in vector field ensembles. *IEEE Trans. Vis. Comput. Graph.* **2016**, *22*, 767–776. [CrossRef] [PubMed]
56. Zhou, L.; Hansen, C.D. A survey of colormaps in visualization. *IEEE Trans. Vis. Comput. Graph.* **2016**, *22*, 2051–2069. [CrossRef] [PubMed]
57. Rhyne, T.-M. *Applying Color Theory to Digital Media and Visualization*, 1st ed.; CRC Press: Boca Raton, FL, USA, 2016; p. 206.
58. Clark, T.L.; Hall, W.D.; Coen, J.L. Source Code Documentation for the Clark-Hall Cloud-Scale Model Code Version G3CH01. NCAR Technical Note NCAR/TN-426+STR. 1996. [CrossRef]
59. Clark, T.L.; Keller, T.; Coen, J.; Neilley, P.; Hsu, H.; Hall, W.D. Terrain-induced Turbulence over Lantau Island: 7 June 1994 Tropical Storm Russ Case Study. *J. Atmos. Sci.* **1997**, *54*, 1795–1814. [CrossRef]
60. Coen, J.L. Simulation of the Big Elk Fire using coupled atmosphere-fire modeling. *Int. J. Wildland Fire* **2005**, *14*, 49–59. [CrossRef]
61. Rothermel, R.C. *A Mathematical Model for Predicting Fire Spread in Wildland Fuels*; Research Paper INT-115; USDA Forest Service, Intermountain Forest and Range Experiment Station: Ogden, UT, USA, 1972.
62. Rothermel, R.C. *Predicting Behavior and Size of Crown Fires in the Northern Rocky Mountains*; Res. Paper INT-438; U.S. Department of Agriculture, Forest Service, Intermountain Forest and Range Experiment Station: Ogden, UT, USA, 1991; p. 46.
63. Albini, F.A. *PROGRAM BURNUP: A Simulation Model of the Burning of Large Woody Natural Fuels*; Final Report on Research Grant INT-92754-GR by USDA Forest Service to Montana State University; Mechanical Engineering Department: Bozeman, MT, USA, 1994.
64. LANDFIRE. (2013, January–last Update). Homepage of the LANDFIRE Project, U.S. Department of Agriculture, Forest Service; U.S. Department of Interior. Available online: http://www.landfire.gov/index.php (accessed on 20 April 2024).
65. Schroeder, W.; Oliva, P.; Giglio, L.; Csiszar, I. The New VIIRS 375 m Active Fire Detection Data Product: Algorithm Description and Initial Assessment. *Remote Sens. Environ.* **2014**, *143*, 85–96. [CrossRef]
66. Schroeder, W.; Oliva, P.; Giglio, L.; Quayle, B.; Lorenz, E.; Morelli, F. Active fire detection using Landsat-8/OLI data. *Remote Sens. Environ.* **2015**, *185*, 210–220. [CrossRef]
67. Coen, J.L.; Schroeder, W.; Quayle, B. The generation and forecast of extreme winds during the origin and progression of the 2017 Tubbs Fire. *Atmosphere* **2018**, *9*, 462. [CrossRef]
68. Incident Information System. Available online: https://inciweb.wildfire.gov/incident-information/catnf-mosquito-fire (accessed on 20 June 2024).

69. Porter, T.W.; Crowfoot, W.; Newsom, G. 2017 Wildfire Activity Statistics. California Department of Forestry and Fire Protection, April 2019. Available online: http://large.stanford.edu/courses/2020/ph240/brown1/docs/redbook-2017.pdf (accessed on 20 June 2024).
70. California Department of Forestry and Fire Protection. Caldor Fire. Available online: https://www.fire.ca.gov/incidents/2021/8/14/caldor-fire/ (accessed on 20 June 2024).
71. Coen, J.L. *Simulation and analysis of the 2021 Caldor Fire*; NSF NCAR: Boulder, CO, USA, 2023; *to be submitted*.
72. University of California San Diego. Alert California. Available online: https://alertcalifornia.org/ (accessed on 20 April 2024).
73. The Mercury News, Map: Homes and Other Buildings Destroyed by the Caldor Fire. 21 August 2021. Available online: https://www.mercurynews.com/2021/08/21/map-caldor-fire-structure-damage/ (accessed on 20 June 2024).
74. Lunder, Z. (Deer Creek Resources, Chico, CA, USA). Personal communication. 2022.